LIMITS OF THE STANDARD MODEL

John Ellis
CERN, Geneva, Switzerland

CERN-TH/2002-320
hep-ph/0211168

Abstract

Supersymmetry is one of the most plausible extensions of the Standard Model, since it is well motivated by the hierarchy problem, supported by measurements of the gauge coupling strengths, consistent with the suggestion from precision electroweak data that the Higgs boson may be relatively light, and provides a ready-made candidate for astrophysical cold dark matter. In the first lecture, constraints on supersymmetric models are reviewed, the problems of fine-tuning the electroweak scale and the dark matter density are discussed, and a number of benchmark scenarios are proposed. Then the prospects for discovering and measuring supersymmetry at the LHC, linear colliders and in non-accelerator experiments are presented. In the second lecture, the evidence for neutrino oscillations is recalled, and the parameter space of the seesaw model is explained. It is shown how these parameters may be explored in a supersymmetric model via the flavour-changing decays and electric dipole moments of charged leptons. It is shown that leptogenesis does not relate the baryon asymmetry of the Universe directly to CP violation in neutrino oscillations. Finally, possible CERN projects beyond the LHC are mentioned.

Lectures given at the PSI Summer School, Zuoz, August 2002

1. Supersymmetry

1.1 Parameters and Problems of the Standard Model

The Standard Model agrees with all confirmed experimental data from accelerators, but is theoretically very unsatisfactory [1]. It does not explain the particle quantum numbers, such as the electric charge Q, weak isospin I, hypercharge Y and colour, and contains at least 19 arbitrary parameters. These include three independent gauge couplings and a possible CP-violating strong-interaction parameter, six quark and three charged-lepton masses, three generalized Cabibbo weak mixing angles and the CP-violating Kobayashi-Maskawa phase, as well as two independent masses for weak bosons.

As if 19 parameters were insufficient to appall you, at least nine more parameters must be introduced to accommodate neutrino oscillations: three neutrino masses, three real mixing angles, and three CP-violating phases, of which one is in principle observable in neutrino-oscillation experiments and the other two in neutrinoless double-beta decay experiments. Even more parameters would be needed to generate masses for all the neutrinos [2], as discussed in Lecture 2.

The Big Issues in physics beyond the Standard Model are conveniently grouped into three categories [1]. These include the problem of **Mass**: what is the origin of particle masses, are they due to a Higgs boson, and, if so, why are the masses so small, **Unification**: is there a simple group framework for unifying all the particle interactions, a so-called Grand Unified Theory (GUT), and **Flavour**: why are there so many different types of quarks and leptons and why do their weak interactions mix in the peculiar way observed? Solutions to all these problems should eventually be incorporated in a Theory of

Everything (TOE) that also includes gravity, reconciles it with quantum mechanics, explains the origin of space-time and why it has four dimensions, etc. String theory, perhaps in its current incarnation of M theory, is the best (only?) candidate we have for such a TOE [3], but we do not yet understand it well enough to make clear experimental predictions.

Supersymmetry is thought to play a rôle in solving many of these problems beyond the Standard Model. The hierarchy of mass scales in physics, and particularly the fact that $m_W \ll m_P$, appears to require relatively light supersymmetric particles: $M \lesssim 1$ TeV for its stabilization [4]. As discussed later, GUT predictions for the unification of gauge couplings work best if the effects of relatively light supersymmetric particles are included [5]. Finally, supersymmetry seems to be essential for the consistency of string theory [6], although this argument does not really restrict the mass scale at which supersymmetric particles should appear.

Thus there are plenty of good reasons to study supersymmetry [7], so this is the subject of Lecture 1, and it reappears in Lecture 2 in connection with the observability of charged-lepton flavour violation.

1.2 Why Supersymmetry?

The main theoretical reason to expect supersymmetry at an accessible energy scale is provided by the *hierarchy problem* [4]: why is $m_W \ll m_P$, or equivalently why is $G_F \sim 1/m_W^2 \gg G_N = 1/m_P^2$? Another equivalent question is why the Coulomb potential in an atom is so much greater than the Newton potential: $e^2 \gg G_N m^2 = m^2/m_P^2$, where m is a typical particle mass?

Your first thought might simply be to set $m_P \gg m_W$ by hand, and forget about the problem. Life is not so simple, because quantum corrections to m_H and hence m_W are quadratically divergent in the Standard Model:

$$\delta m_{H,W}^2 \simeq \mathcal{O}(\frac{\alpha}{\pi})\Lambda^2, \tag{1}$$

which is $\gg m_W^2$ if the cutoff Λ, which represents the scale where new physics beyond the Standard Model appears, is comparable to the GUT or Planck scale. For example, if the Standard Model were to hold unscathed all the way up the Planck mass $m_P \sim 10^{19}$ GeV, the radiative correction (1) would be 36 orders of magnitude greater than the physical values of $m_{H,W}^2$!

In principle, this is not a problem from the mathematical point of view of renormalization theory. All one has to do is postulate a tree-level value of m_H^2 that is (very nearly) equal and opposite to the 'correction' (1), and the correct physical value may be obtained. However, this fine tuning strikes many physicists as rather unnatural: they would prefer a mechanism that keeps the 'correction' (1) comparable at most to the physical value [4].

This is possible in a supersymmetric theory, in which there are equal numbers of bosons and fermions with identical couplings. Since bosonic and fermionic loops have opposite signs, the residual one-loop correction is of the form

$$\delta m_{H,W}^2 \simeq \mathcal{O}(\frac{\alpha}{\pi})(m_B^2 - m_F^2), \tag{2}$$

which is $\lesssim m_{H,W}^2$ and hence naturally small if the supersymmetric partner bosons B and fermions F have similar masses:

$$|m_B^2 - m_F^2| \lesssim 1 \text{ TeV}^2. \tag{3}$$

This is the best motivation we have for finding supersymmetry at relatively low energies [4]. In addition to this first supersymmetric miracle of removing (2) the quadratic divergence (1), many logarithmic divergences are also absent in a supersymmetric theory [8], a property that also plays a rôle in the construction of supersymmetric GUTs [1].

Could any of the known particles in the Standard Model be paired up in supermultiplets? Unfortunately, none of the known fermions q, ℓ can be paired with any of the 'known' bosons $\gamma, W^\pm Z^0, g, H$,

because their internal quantum numbers do not match [9]. For example, quarks q sit in triplet representations of colour, whereas the known bosons are either singlets or octets of colour. Then again, leptons ℓ have non-zero lepton number $L = 1$, whereas the known bosons have $L = 0$. Thus, the only possibility seems to be to introduce new supersymmetric partners (spartners) for all the known particles: quark $\rightarrow$ squark, lepton $\rightarrow$ slepton, photon $\rightarrow$ photino, Z $\rightarrow$ Zino, W $\rightarrow$ Wino, gluon $\rightarrow$ gluino, Higgs $\rightarrow$ Higgsino. The best that one can say for supersymmetry is that it economizes on principle, not on particles!

1.3 Hints of Supersymmetry

There are some phenomenological hints that supersymmetry may, indeed, appear at the Tev scale. One is provided by the strengths of the different gauge interactions, as measured at LEP [5]. These may be run up to high energy scales using the renormalization-group equations, to see whether they unify as predicted in a GUT. The answer is no, if supersymmetry is not included in the calculations. In that case, GUTs would require

$$\sin^2\theta_W \;=\; 0.214 \pm 0.004, \tag{4}$$

whereas the experimental value of the effective neutral weak mixing parameter at the Z^0 peak is $\sin^2\theta = 0.23149 \pm 0.00017$ [10]. On the other hand, minimal supersymmetric GUTs predict

$$\sin^2\theta_W \;\simeq\; 0.232, \tag{5}$$

where the error depends on the assumed sparticle masses, the preferred value being around 1 TeV [5], as suggested completely independently by the naturalness of the electroweak mass hierarchy.

A second hint is the fact that precision electroweak data prefer a relatively light Higgs boson weighing less than about 200 GeV [10]. This is perfectly consistent with calculations in the minimal supersymmetric extension of the Standard Model (MSSM), in which the lightest Higgs boson weighs less than about 130 GeV [11].

A third hint is provided by the astrophysical necessity of cold dark matter. This could be provided by a neutral, weakly-interacting particle weighing less than about 1 TeV, such as the lightest supersymmetric particle (LSP) χ [12].

1.4 Building Supersymmetric Models

Any supersymmetric model is based on a Lagrangian that contains a supersymmetric part and a supersymmetry-breaking part [13, 7]:

$$\mathcal{L} \;=\; \mathcal{L}_{susy} \;+\; \mathcal{L}_{susy\times}. \tag{6}$$

We concentrate here on the supersymmetric part $\mathcal{L}_{susy}$. The minimal supersymmetric extension of the Standard Model (MSSM) has the same gauge interactions as the Standard Model, and Yukawa interactions that are closely related. They are based on a superpotential W that is a cubic function of complex superfields corresponding to left-handed fermion fields. Conventional left-handed lepton and quark doublets are denoted L, Q, and right-handed fermions are introduced via their conjugate fields, which are left-handed, $e_R \rightarrow E^c, u_R \rightarrow U^c, d_R \rightarrow D^c$. In terms of these,

$$W \;=\; \Sigma_{L,E^c}\lambda_L L E^c H_1 \;+\; \Sigma_{Q,U^c}\lambda_U Q U^c H_2 \;+\; \Sigma_{Q,D^c}\lambda_D Q D^c H_1 \;+\mu H_1 H_2. \tag{7}$$

A few words of explanation are warranted. The first three terms in (7) yield masses for the charged leptons, charge-$(+2/3)$ quarks and charge-$(-1/3)$ quarks respectively. All of the Yukawa couplings $\lambda_{L,U,D}$ are 3×3 matrices in flavour space, whose diagonalizations yield the mass eigenstates and Cabibbo-Kobayashi-Maskawa mixing angles for quarks.

Note that two distinct Higgs doublets $H_{1,2}$ have been introduced, for two important reasons. One reason is that the superpotential must be an analytic polynomial: it cannot contain both H and H^*,

whereas the Standard Model uses both of these to give masses to all the quarks and leptons with just a single Higgs doublet. The other reason for introducing two Higgs doublets $H_{1,2}$ is to cancel the triangle anomalies that destroy the renormalizability of a gauge theory. Ordinary Higgs boson doublets do not contribute to these anomalies, but the fermions in Higgs supermultiplets do, and pairs of doublets are required to cancel each others' contributions. Once two Higgs supermultiplets have been introduced, there must in general be a bilinear term $\mu H_1 H_2$ coupling them together.

In general, the supersymmetric partners of the $W^\pm$ and charged Higgs bosons $H^\pm$ (the 'charginos' $\chi^\pm$) mix, as do those of the γ, Z^0 and $H^0_{1,2}$ (the 'neutralinos' χ^0_i): see [1]. The lightest neutralino χ is a likely candidate to be the Lightest Supersymmetric Particle (LSP), and hence constitute the astrophysical cold dark matter [12].

Once the MSSM superpotential (7) has been specified, the effective potential is also fixed:

$$V \; = \; \Sigma_i |F^i|^2 \; + \; \frac{1}{2}\Sigma_a (D^a)^2 : \quad F_i^* \equiv \frac{\partial W}{\partial \phi^i}, \; D^a \equiv g_a \phi_i^* (T^a)^i_j \phi^j, \tag{8}$$

where the sums run over the different chiral fields i and the $SU(3), SU(2)$ and $U(1)$ gauge-group factors a. Thus, the quartic terms in the effective Higgs potential are completely fixed, which leads to the prediction that the lightest Higgs boson should weigh $\lesssim 130$ GeV [11].

In addition to the supersymmetric part $\mathcal{L}_{susy}$ of the lagrangian (6) above, there is also the superymmetry-breaking piece $\mathcal{L}_{susy\times}$. The origin of this piece is unclear, and in these lectures we shall just assume a suitable phenomenological parameterization. In order not to undo the supersymmetric miracles mentioned above, the breaking of supersymmetry should be 'soft', in the sense that it does not reintroduce any unwanted quadratic or logarithmic divergences. The candidates for such soft superymmetry breaking are gaugino masses M_a for each of the gauge group factors a in the Standard Model, scalar masses-squared m_0^2 that should be regarded as matrices in the flavour index i of the matter supermultiplets, and trilinear scalar couplings A_{ijk} corresponding to each of the Yukawa couplings λ_{ijk} in the Standard Model.

There are very many such soft superymmetry-breaking terms. Upper limits on flavour-changing neutral interactions suggest [14] that the scalar masses-squared m_0^2 are (approximately) independent of generation for particles with the same quantum numbers, e.g., sleptons, and that the A_{ijk} are related to the λ_{ijk} by a universal constant of proportionality A. In these lectures, for definiteness, we assume universality at the input GUT scale for all the gaugino masses:

$$M_a \; = \; m_{1/2}, \tag{9}$$

and likewise for the scalar masses-squared and trilinear parameters:

$$m_0^2 \; = m_0^2 \delta^i_j, \; A_{ijk} \; = \; A\lambda_{ijk}. \tag{10}$$

This is known as the constrained MSSM (CMSSM). The values of the soft supersymmetry-breaking parameters at observable energies $\sim$ 1 TeV are renormalized by calculable factors [15], in a similar manner to the gauge couplings and fermion masses. These renormalization factors are included in the subsequent discussions, and play a key rôle in Lecture 2. The physical value of μ is fixed up to a sign in the CMSSM, as is the pseudoscalar Higgs mass m_A, by the electroweak vacuum conditions.

1.5 Constraints on the MSSM

Important experimental constraints on the MSSM parameter space are provided by direct searches at LEP and the Tevatron collider, as compiled in the $(m_{1/2}, m_0)$ planes for different values of $\tan\beta$ and the sign of μ in Fig. 1. One of these is the limit $m_{\chi^\pm} \gtrsim 103.5$ GeV provided by chargino searches at LEP [16], where the fourth significant figure depends on other CMSSM parameters. LEP has also provided lower limits on slepton masses, of which the strongest is $m_{\tilde{e}} \gtrsim 99$ GeV [17], again depending

only sightly on the other CMSSM parameters, as long as $m_{\tilde{e}} - m_\chi \gtrsim 10$ GeV. The most important constraints on the u, d, s, c, b squarks and gluinos are provided by the FNAL Tevatron collider: for equal masses $m_{\tilde{q}} = m_{\tilde{g}} \gtrsim 300$ GeV. In the case of the $\tilde{t}$, LEP provides the most stringent limit when $m_{\tilde{t}} - m_\chi$ is small, and the Tevatron for larger $m_{\tilde{t}} - m_\chi$ [16].

Another important constraint is provided by the LEP lower limit on the Higgs mass: $m_H > 114.4$ GeV [19]. This holds in the Standard Model, for the lightest Higgs boson h in the general MSSM for $\tan\beta \lesssim 8$, and almost always in the CMSSM for all $\tan\beta$, at least as long as CP is conserved [1]. Since m_h is sensitive to sparticle masses, particularly $m_{\tilde{t}}$, via loop corrections:

$$\delta m_h^2 \propto \frac{m_t^4}{m_W^2} \ln\left(\frac{m_{\tilde{t}}^2}{m_t^2}\right) + \ldots \tag{11}$$

the Higgs limit also imposes important constraints on the soft supersymmetry-breaking CMSSM parameters, principally $m_{1/2}$ [23] as seen in Fig. 1. The constraints are here evaluated using `FeynHiggs` [24], which is estimated to have a residual uncertainty of a couple of GeV in m_h.

Also shown in Fig. 1 is the constraint imposed by measurements of $b \to s\gamma$ [20]. These agree with the Standard Model, and therefore provide bounds on MSSM particles, such as the chargino and charged Higgs masses, in particular. Typically, the $b \to s\gamma$ constraint is more important for $\mu < 0$, as seen in Fig. 1a and c, but it is also relevant for $\mu > 0$, particularly when $\tan\beta$ is large as seen in Fig. 1d.

The final experimental constraint we consider is that due to the measurement of the anomolous magnetic moment of the muon. Following its first result last year [25], the BNL E821 experiment has recently reported a new measurement [26] of $a_\mu \equiv \frac{1}{2}(g_\mu - 2)$, which deviates by 3.0 standard deviations from the best available Standard Model predictions based on low-energy $e^+e^- \to$ hadrons data [27]. On the other hand, the discrepancy is more like 1.6 standard deviations if one uses $\tau \to$ hadrons data to calculate the Standard Model prediction. Faced with this confusion, and remembering the chequered history of previous theoretical calculations [28], it is reasonable to defer judgement whether there is a significant discrepancy with the Standard Model. However, either way, the measurement of a_μ is a significant constraint on the CMSSM, favouring $\mu > 0$ in general, and a specific region of the $(m_{1/2}, m_0)$ plane if one accepts the theoretical prediction based on $e^+e^- \to$ hadrons data [29]. The regions preferred by the current $g-2$ experimental data and the $e^+e^- \to$ hadrons data are shown in Fig. 1.

Fig. 1 also displays the regions where the supersymmetric relic density $\rho_\chi = \Omega_\chi \rho_{critical}$ falls within the preferred range

$$0.1 < \Omega_\chi h^2 < 0.3 \tag{12}$$

The upper limit on the relic density is rigorous, since astrophysics and cosmology tell us that the total matter density $\Omega_m \lesssim 0.4$ [30], and the Hubble expansion rate $h \sim 1/\sqrt{2}$ to within about 10 % (in units of 100 km/s/Mpc). On the other hand, the lower limit in (12) is optional, since there could be other important contributions to the overall matter density. Smaller values of $\Omega_\chi h^2$ correspond to smaller values of $(m_{1/2}, m_0)$, in general.

As is seen in Fig. 1, there are generic regions of the CMSSM parameter space where the relic density falls within the preferred range (12). What goes into the calculation of the relic density? It is controlled by the annihilation cross section [12]:

$$\rho_\chi = m_\chi n_\chi\,, \quad n_\chi \sim \frac{1}{\sigma_{ann}(\chi\chi \to \ldots)}\,, \tag{13}$$

where the typical annihilation cross section $\sigma_{ann} \sim 1/m_\chi^2$. For this reason, the relic density typically increases with the relic mass, and this combined with the upper bound in (12) then leads to the common expectation that $m_\chi \lesssim \mathcal{O}(1)$ GeV.

[1] The lower bound on the lightest MSSM Higgs boson may be relaxed significantly if CP violation feeds into the MSSM Higgs sector [22].

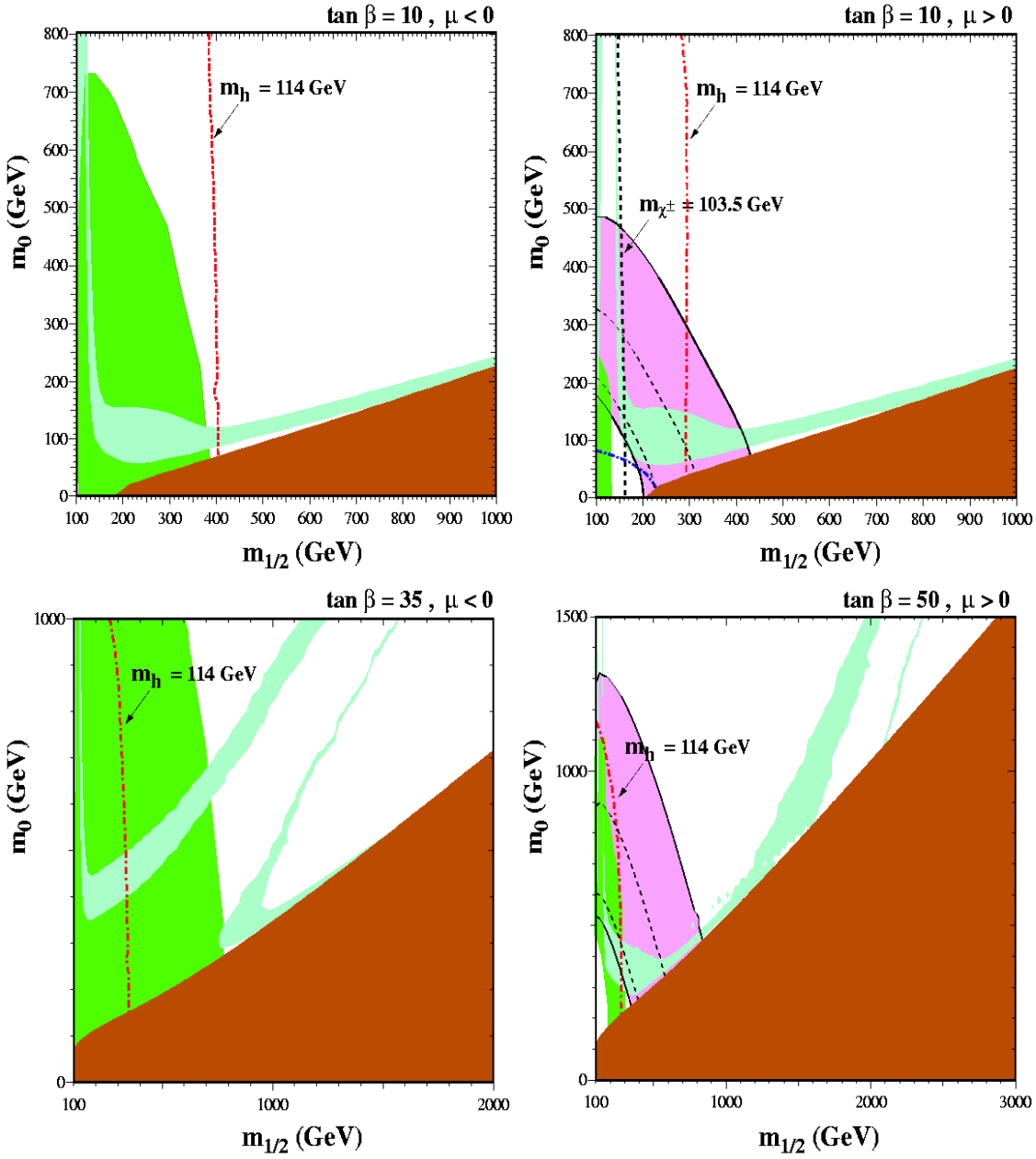

Fig. 1: *Compilations of phenomenological constraints on the CMSSM for (a)* $\tan\beta = 10, \mu < 0$, *(b)* $\tan\beta = 10, \mu > 0$, *(c)* $\tan\beta = 35, \mu < 0$ *and (d)* $\tan\beta = 50, \mu > 0$, *assuming* $A_0 = 0, m_t = 175$ *GeV and* $m_b(m_b)^{\overline{MS}}_{SM} = 4.25$ *GeV [18]. The near-vertical lines are the LEP limits* $m_{\chi^\pm} = 103.5$ *GeV (dashed and black) [16], shown in (b) only, and* $m_h = 114$ *GeV (dotted and red) [19]. Also, in the lower left corner of (b), we show the* $m_{\tilde{e}} = 99$ *GeV contour [17]. In the dark (brick red) shaded regions, the LSP is the charged* $\tilde{\tau}_1$*, so this region is excluded. The light (turquoise) shaded areas are the cosmologically preferred regions with* $0.1 \leq \Omega_\chi h^2 \leq 0.3$ *[18]. The medium (dark green) shaded regions that are most prominent in panels (a) and (c) are excluded by* $b \to s\gamma$ *[20]. The shaded (pink) regions in the upper right regions show the* $\pm 2\,\sigma$ *ranges of* $g_\mu - 2$*. For* $\mu > 0$*, the* $\pm 2(1)\,\sigma$ *contours are also shown as solid (dashed) black lines [21].*

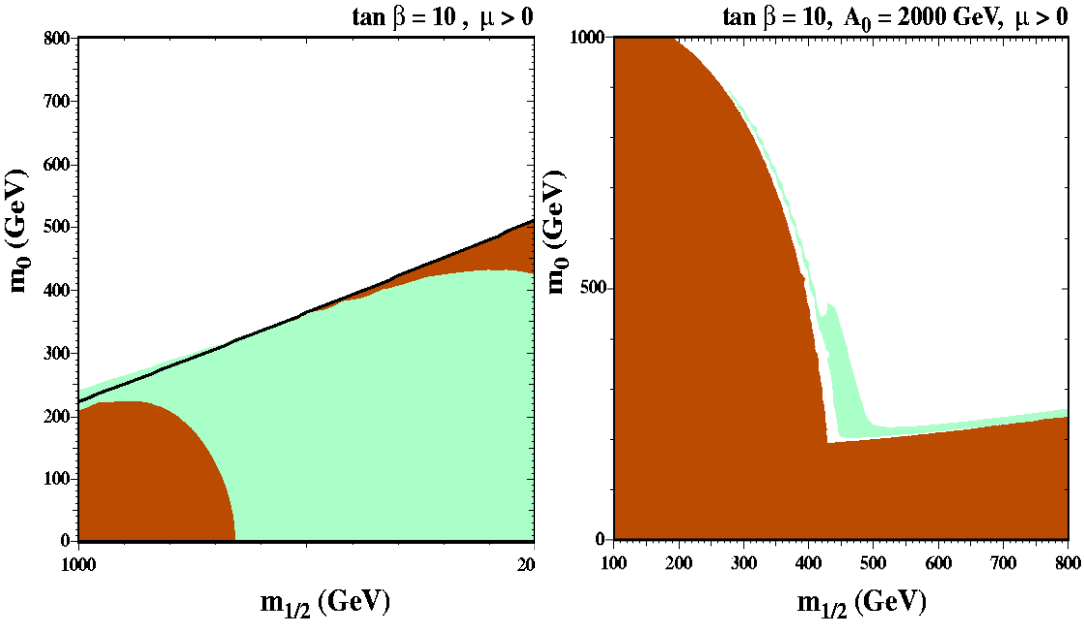

Fig. 2: *(a) The large-$m_{1/2}$ 'tail' of the $\chi - \tilde{\tau}_1$ coannihilation region for $\tan\beta = 10$, $A = 0$ and $\mu < 0$ [32], superimposed on the disallowed dark (brick red) shaded region where $m_{\tilde{\tau}_1} < m_\chi$, and (b) the $\chi - \tilde{t}_1$ coannihilation region for $\tan\beta = 10$, $A = 2000$ GeV and $\mu > 0$ [34], exhibiting a large-m_0 'tail', again with a dark (brick red) shaded region excluded because the LSP is charged.*

However, there are various ways in which the generic upper bound on m_χ can be increased along filaments in the $(m_{1/2}, m_0)$ plane. For example, if the next-to-lightest sparticle (NLSP) is not much heavier than χ: $\Delta m/m_\chi \lesssim 0.1$, the relic density may be suppressed by coannihilation: $\sigma(\chi + \text{NLSP} \to \ldots)$ [31]. In this way, the allowed CMSSM region may acquire a 'tail' extending to larger sparticle masses. An example of this possibility is the case where the NLSP is the lighter stau: $\tilde{\tau}_1$ and $m_{\tilde{\tau}_1} \sim m_\chi$, as seen in Figs. 1(a) and (b) and extended to larger $m_{1/2}$ in Fig. 2(a) [32]. Another example is coannihilation when the NLSP is the lighter stop [33], $\tilde{t}_1$, and $m_{\tilde{t}_1} \sim m_\chi$, which may be important in the general MSSM or in the CMSSM when A is large, as seen in Fig. 2(b) [34]. In the cases studied, the upper limit on m_χ is not affected by stop coannihilation.

Another mechanism for extending the allowed CMSSM region to large m_χ is rapid annihilation via a direct-channel pole when $m_\chi \sim \frac{1}{2} m_{Higgs,Z}$ [35, 18]. This may yield a 'funnel' extending to large $m_{1/2}$ and m_0 at large $\tan\beta$, as seen in panels (c) and (d) of Fig. 1 [18]. Yet another allowed region at large $m_{1/2}$ and m_0 is the 'focus-point' region [36], which is adjacent to the boundary of the region where electroweak symmetry breaking is possible, as seen in Fig. 3. The lightest supersymmetric particle is relatively light in this region.

1.6 Fine Tuning

The above-mentioned filaments extending the preferred CMSSM parameter space are clearly exceptional in some sense, so it is important to understand the sensitivity of the relic density to input parameters, unknown higher-order effects, etc. One proposal is the relic-density fine-tuning measure [37]

$$\Delta^\Omega \equiv \sqrt{\sum_i \left(\frac{\partial \ln(\Omega_\chi h^2)}{\partial \ln a_i} \right)^2} \tag{14}$$

where the sum runs over the input parameters, which might include (relatively) poorly-known Standard Model quantities such as m_t and m_b, as well as the CMSSM parameters $m_0, m_{1/2}$, etc. As seen in Fig. 4, the sensitivity Δ^Ω (14) is relatively small in the 'bulk' region at low $m_{1/2}$, m_0, and $\tan\beta$. However, it

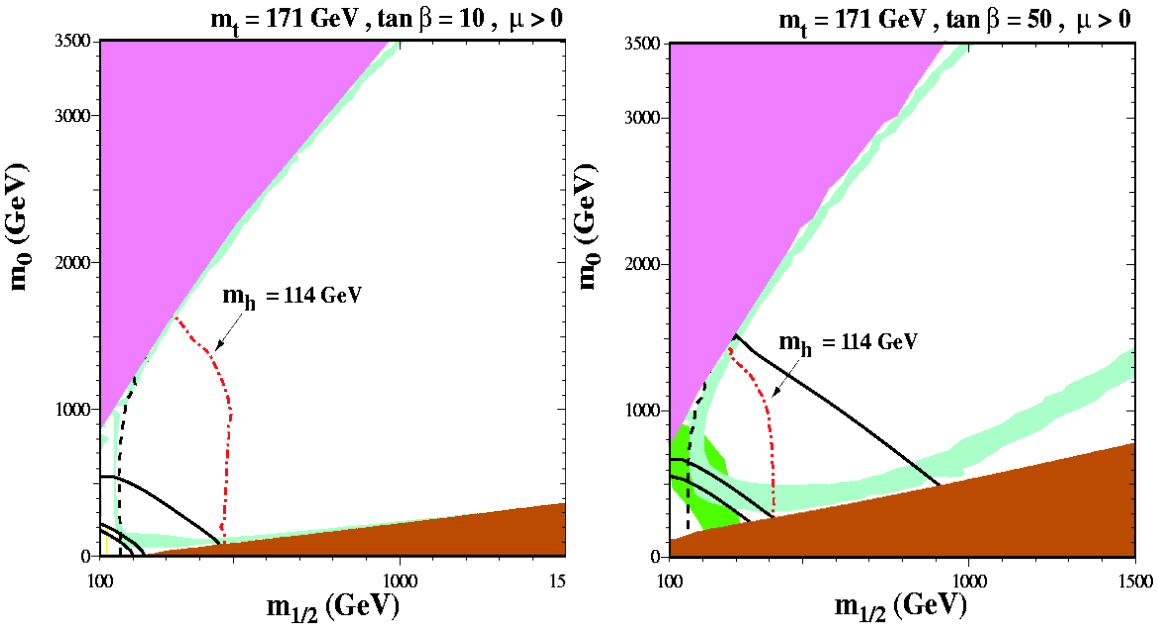

Fig. 3: *An expanded view of the $m_{1/2} - m_0$ parameter plane showing the focus-point regions [36] at large m_0 for (a) $tan\beta = 10$, and (b) $\tan\beta = 50$ [21]. In the shaded (mauve) region in the upper left corner, there are no solutions with proper electroweak symmetry breaking, so these are excluded in the CMSSM. Note that we have chosen $m_t = 171$ GeV, in which case the focus-point region is at lower m_0 than when $m_t = 175$ GeV, as assumed in the other figures. The position of this region is very sensitive to m_t. The black contours (both dashed and solid) are as in Fig. 1, we do not shade the preferred $g - 2$ region.*

is somewhat higher in the $\chi - \tilde{\tau}_1$ coannihilation 'tail', and at large $\tan\beta$ in general. The sensitivity measure Δ^{Ω} (14) is particularly high in the rapid-annihilation 'funnel' and in the 'focus-point' region. This explains why published relic-density calculations may differ in these regions [38], whereas they agree well when Δ^{Ω} is small: differences may arise because of small differences in the values and treatments of the inputs.

It is important to note that the relic-density fine-tuning measure (14) is distinct from the traditional measure of the fine-tuning of the electroweak scale [39]:

$$\Delta = \sqrt{\sum_i \Delta_i^2}, \quad \Delta_i \equiv \frac{\partial \ln m_W}{\partial \ln a_i} \tag{15}$$

Sample contours of the electroweak fine-tuning measure are shown (15) are shown in Figs. 5 [34]. This electroweak fine tuning is logically different from the cosmological fine tuning, and values of Δ are not necessarily related to values of Δ^{Ω}, as is apparent when comparing the contours in Figs. 4 and 5. Electroweak fine-tuning is sometimes used as a criterion for restricting the CMSSM parameters. However, the interpretation of Δ (15) is unclear. How large a value of Δ is tolerable? Different people may well have different pain thresholds. Moreover, correlations between input parameters may reduce its value in specific models, and the regions allowed by the different constraints can become very different when we relax some of the CMSSM assumptions, e.g., the universality between the input Higgs masses and those of the squarks and sleptons, a subject beyond the scope of these Lectures.

1.7 Benchmark Supersymmetric Scenarios

As seen in Fig. 1, all the experimental, cosmological and theoretical constraints on the MSSM are mutually compatible. As an aid to understanding better the physics capabilities of the LHC, various e^+e^- linear collider designs and non-accelerator experiments, a set of benchmark supersymmetric scenarios

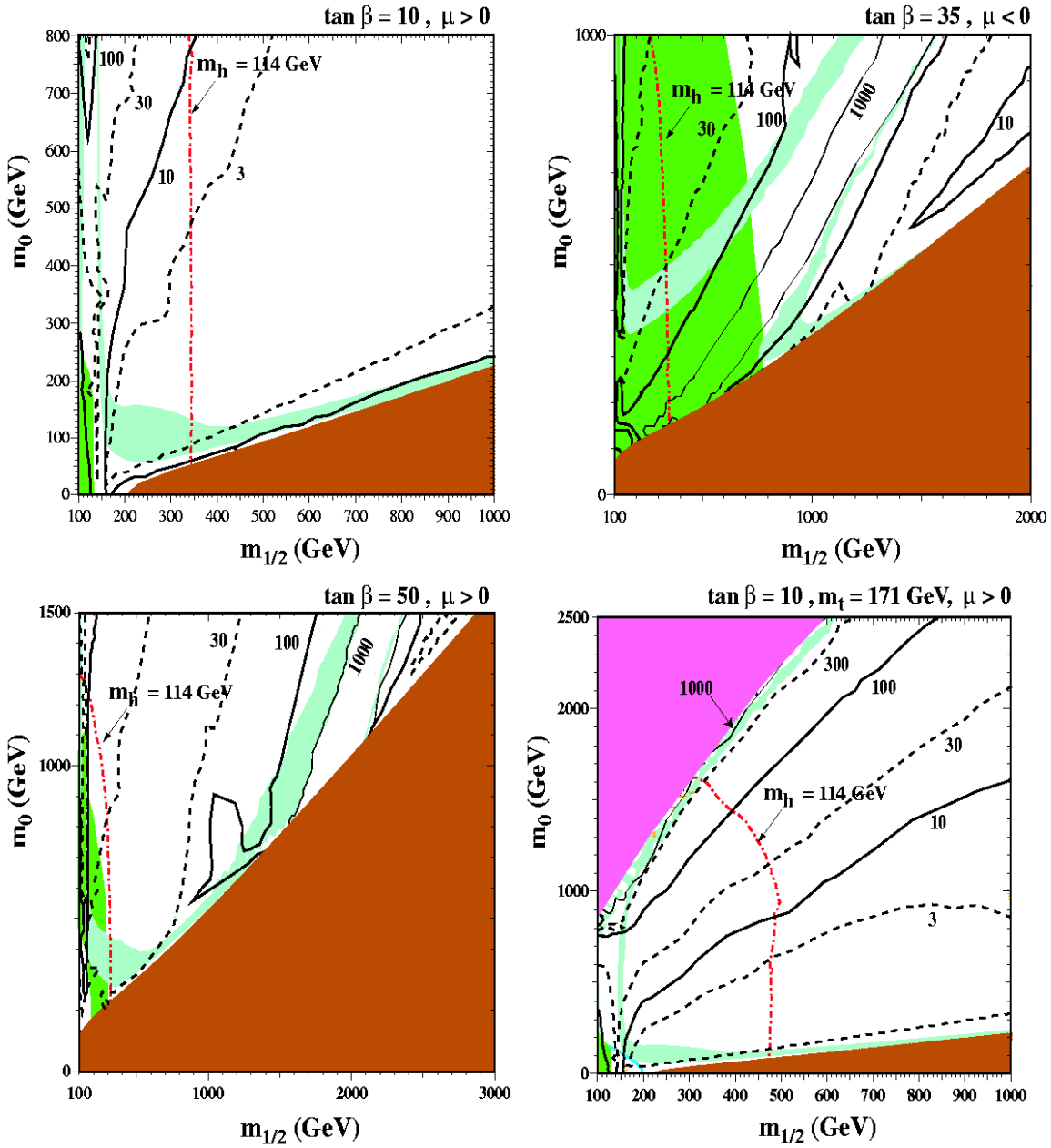

Fig. 4: *Contours of the total sensitivity Δ^{Ω} (14) of the relic density in the $(m_{1/2}, m_0)$ planes for (a) $\tan\beta = 10, \mu > 0, m_t = 175$ GeV, (b) $\tan\beta = 35, \mu < 0, m_t = 175$ GeV, (c) $\tan\beta = 50, \mu > 0, m_t = 175$ GeV, and (d) $\tan\beta = 10, \mu > 0, m_t = 171$ GeV, all for $A_0 = 0$ [37]. The light (turquoise) shaded areas are the cosmologically preferred regions with $0.1 \leq \Omega_\chi h^2 \leq 0.3$. In the dark (brick red) shaded regions, the LSP is the charged $\tilde{\tau}_1$, so these regions are excluded. In panel (d), the medium shaded (mauve) region is excluded by the electroweak vacuum conditions.*

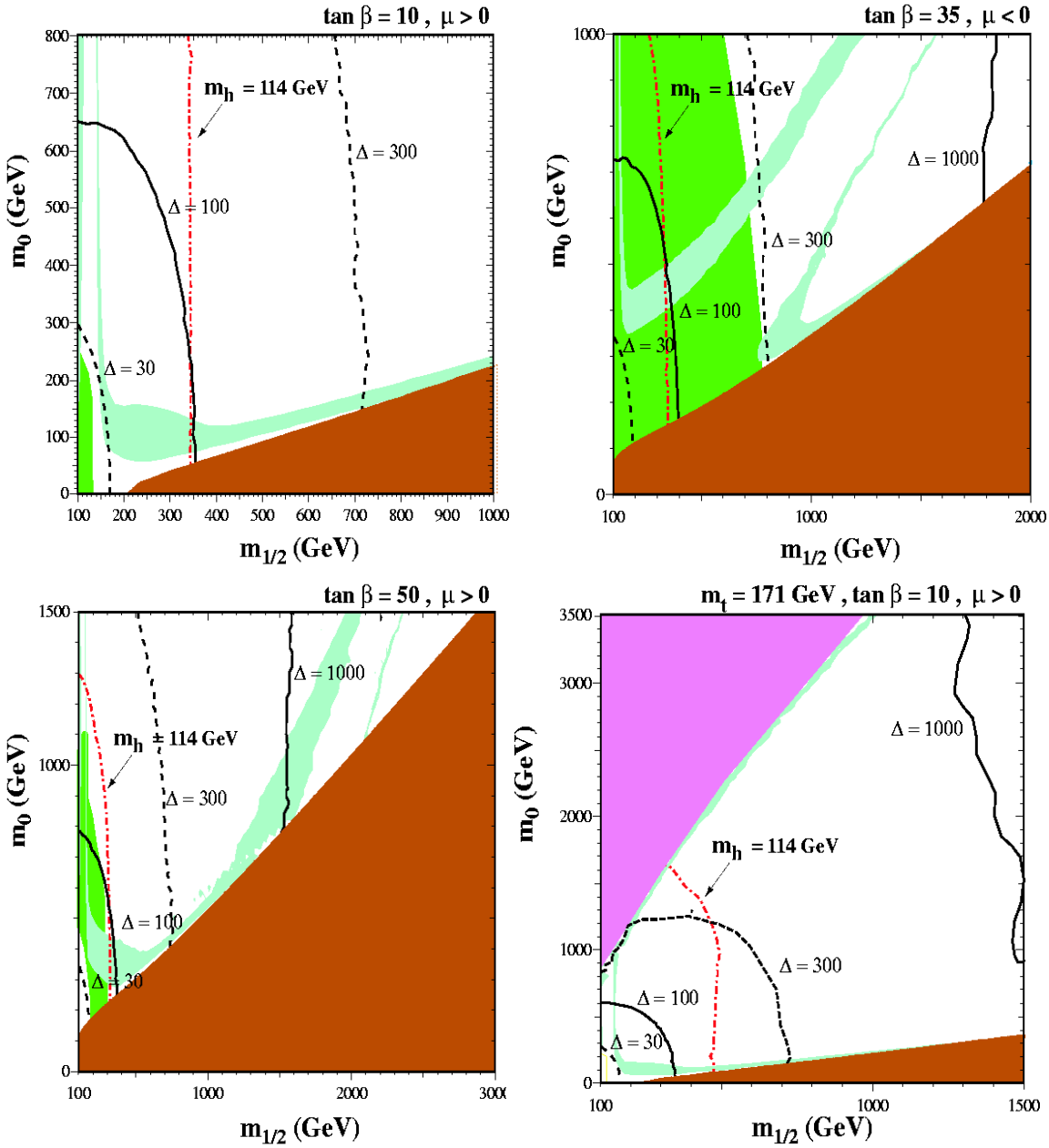

Fig. 5: *Contours of the electroweak fine-tuning measure* Δ *(15) in the* $(m_{1/2}, m_0)$ *planes for (a)* $\tan\beta = 10, \mu > 0, m_t = 175$ *GeV, (b)* $\tan\beta = 35, \mu < 0, m_t = 175$ *GeV, (c)* $\tan\beta = 50, \mu > 0, m_t = 175$ *GeV, and (d)* $\tan\beta = 10, \mu > 0, m_t = 171$ *GeV, all for* $A_0 = 0$ *[21]. The light (turquoise) shaded areas are the cosmologically preferred regions with* $0.1 \leq \Omega_\chi h^2 \leq 0.3$*. In the dark (brick red) shaded regions, the LSP is the charged* $\tilde{\tau}_1$*, so this region is excluded. In panel (d), the medium shaded (mauve) region is excluded by the electroweak vacuum conditions.*

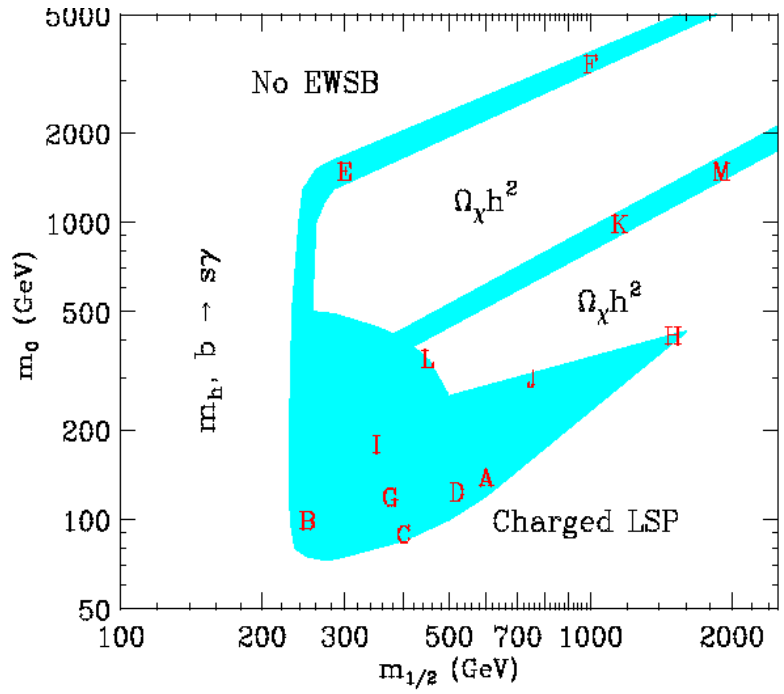

Fig. 6: *The locations of the benchmark points proposed in [40] in the region of the* $(m_{1/2}, m_0)$ *plane where* $\Omega_\chi h^2$ *falls within the range preferred by cosmology (shaded blue). Note that the filaments of the allowed parameter space extending to large* $m_{1/2}$ *and/or* m_0 *are sampled.*

have been proposed [40]. Their distribution in the $(m_{1/2}, m_0)$ plane is sketched in Fig. 6. These benchmark scenarios are compatible with all the accelerator constraints mentioned above, including the LEP searches and $b \to s\gamma$, and yield relic densities of LSPs in the range suggested by cosmology and astrophysics. The benchmarks are not intended to sample 'fairly' the allowed parameter space, but rather to illustrate the range of possibilities currently allowed.

In addition to a number of benchmark points falling in the 'bulk' region of parameter space at relatively low values of the supersymmetric particle masses, as see in Fig. 6, we also proposed [40] some points out along the 'tails' of parameter space extending out to larger masses. These clearly require some degree of fine-tuning to obtain the required relic density and/or the correct $W^\pm$ mass, and some are also disfavoured by the supersymmetric interpretation of the $g_\mu - 2$ anomaly, but all are logically consistent possibilities.

1.8 Prospects for Discovering Supersymmetry

In the CMSSM discussed here, there are just a few prospects for discovering supersymmetry at the FNAL *Tevatron collider* [40], but these could be increased in other supersymmetric models [41]. Fig. 7 shows the physics reach for observing pairs of supersymmetric particles at the *LHC*. The signature for supersymmetry - multiple jets (and/or leptons) with a large amount of missing energy - is quite distinctive, as seen in Fig. 8 [42, 43]. Therefore, the detection of the supersymmetric partners of quarks and gluons at the LHC is expected to be quite easy if they weigh less than about 2.5 TeV [44]. Moreover, in many scenarios one should be able to observe their cascade decays into lighter supersymmetric particles, as seen in Fig. 9 [45]. As seen in Fig. 10, large fractions of the supersymmetric spectrum should be seen in most of the benchmark scenarios, although there are a couple where only the lightest supersymmetric Higgs boson would be seen [40], as seen in Fig. 10.

Electron-positron colliders provide very clean experimental environments, with egalitarian production of all the new particles that are kinematically accessible, including those that have only weak

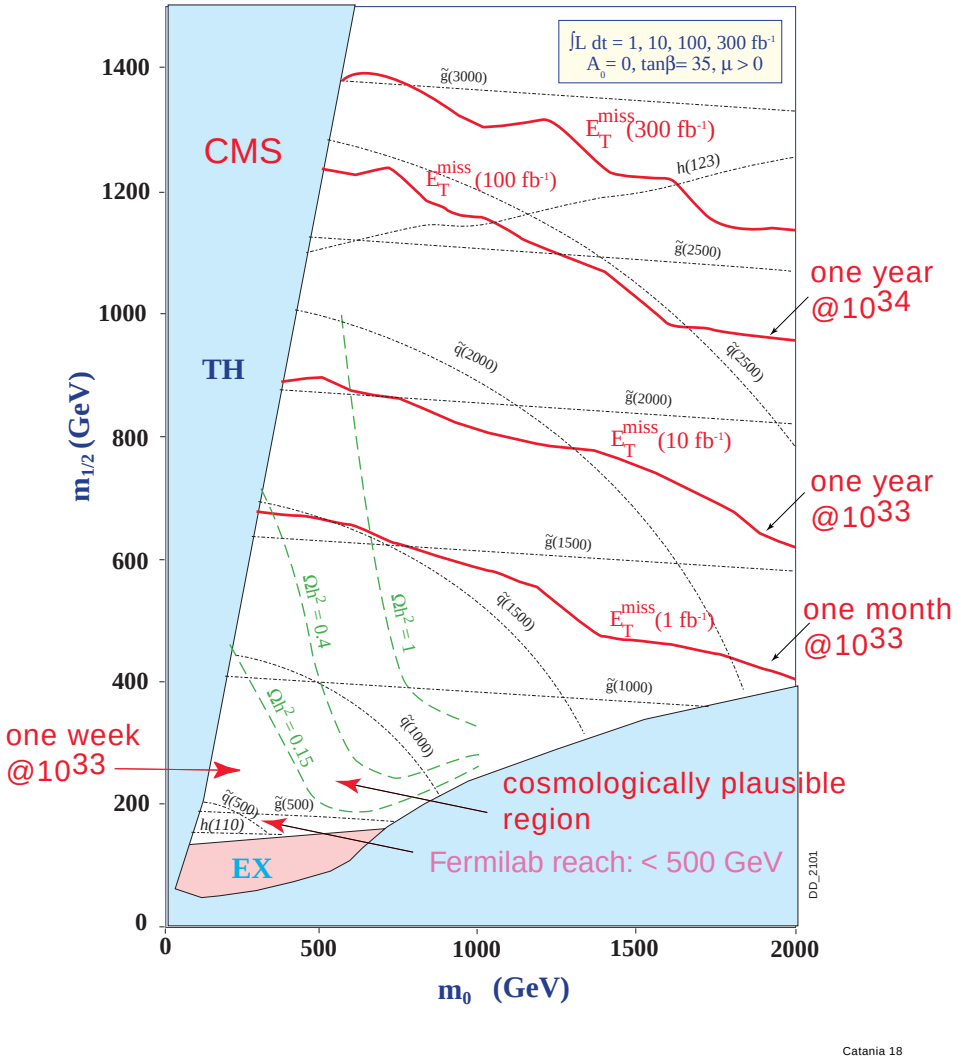

Catania 18

Fig. 7: *The regions of the* $(m_0, m_{1/2})$ *plane that can be explored by the LHC with various integrated luminosities [44], using the missing energy + jets signature [43].*

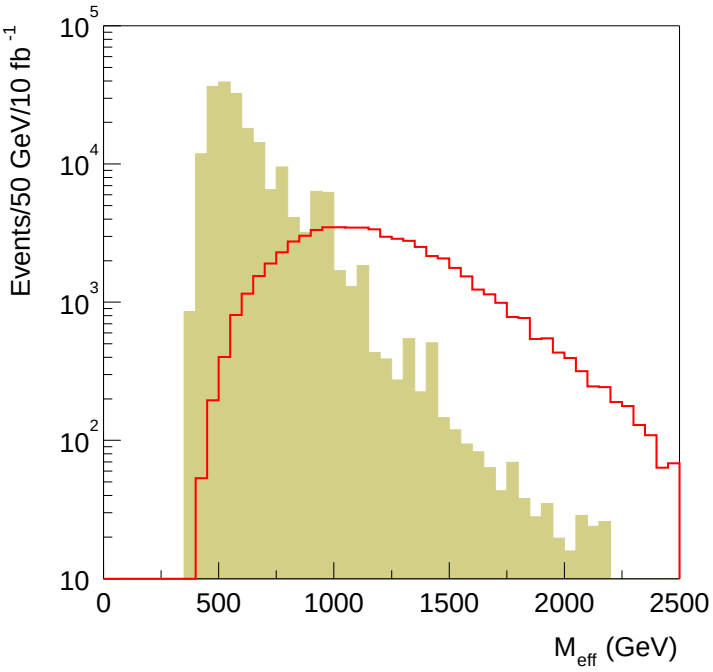

Fig. 8: *The distribution expected at the LHC in the variable $M_{\rm eff}$ that combines the jet energies with the missing energy [46, 42, 43].*

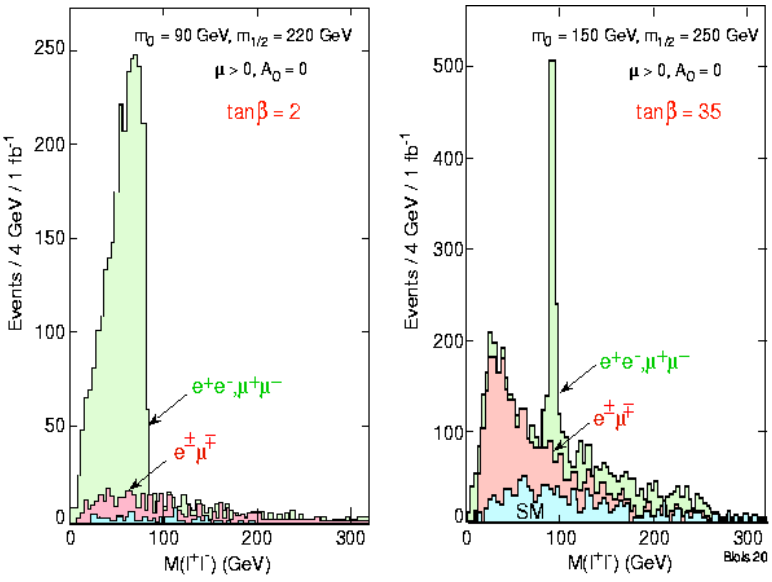

Fig. 9: *The dilepton mass distributions expected at the LHC due to sparticle decays in two different supersymmetric scenarios [46, 44, 43].*

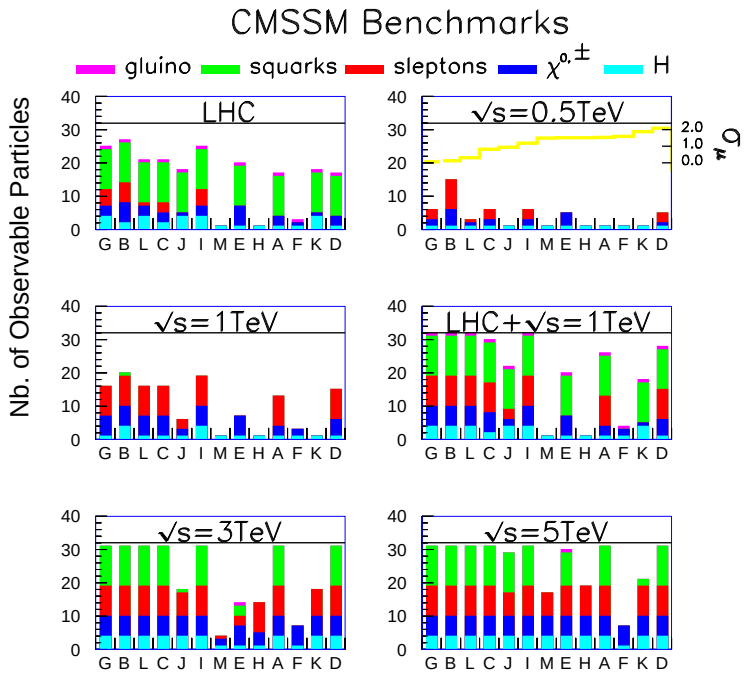

Fig. 10: *The numbers of different sparticles expected to be observable at the LHC and/or linear e^+e^- colliders with various energies, in each of the proposed benchmark scenarios [40], ordered by their difference from the present central experimental value of $g_\mu - 2$.*

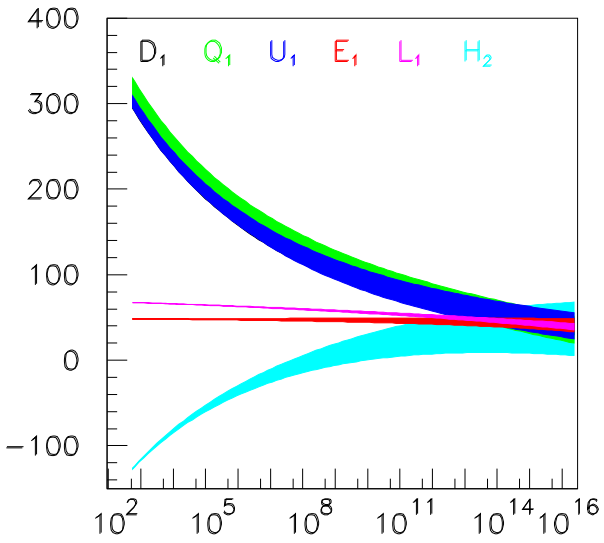

Fig. 11: *Measurements of sparticle masses at the LHC and a linear e^+e^- linear collider will enable one to check their universality at some input GUT scale, and check possible models of supersymmetry breaking [50]. Both axes are labelled in GeV units.*

interactions. Moreover, polarized beams provide a useful analysis tool, and $e\gamma$, $\gamma\gamma$ and e^-e^- colliders are readily available at relatively low marginal costs.

The $e^+e^- \to \bar{t}t$ threshold is known to be at $E_{\rm CM} \sim 350$ GeV. Moreover, if the Higgs boson indeed weighs less than 200 GeV, as suggested by the precision electroweak data, its production and study would also be easy at an e^+e^- collider with $E_{\rm CM} \sim 500$ GeV. With a luminosity of 10^{34} cm^{-2}s^{-1} or more, many decay modes of the Higgs boson could be measured very accurately, and one might be able to find a hint whether its properties were modified by supersymmetry [47, 48].

However, the direct production of supersymmetric particles at such a collider cannot be guaranteed [49]. We do not yet know what the supersymmetric threshold energy may be (or even if there is one!). We may well not know before the operation of the LHC, although $g_\mu - 2$ might provide an indication [29], if the uncertainties in the Standard Model calculation can be reduced.

If an e^+e^- collider is above the supersymmetric threshold, it will be able to measure very accurately the sparticle masses. By comparing their masses with those of different sparticles produced at the LHC, one would be able to make interesting tests of string and GUT models of supersymmetry breaking, as seen in Fig. 11 [50]. However, independently from the particular benchmark scenarios proposed, a linear e^+e^- collider with $E_{\rm CM} < 1$ TeV would not cover all the supersymmetric parameter space allowed by cosmology [49, 40].

Nevertheless, there are compelling physics arguments for such a linear e^+e^- collider, which would be very complementary to the LHC in terms of its exploratory power and precision [47]. It is to be hoped that the world community will converge on a single project with the widest possible energy range.

CERN and collaborating institutes are studying the possible following step in linear e^+e^- colliders, a multi-TeV machine called CLIC [51, 52]. This would use a double-beam technique to attain accelerating gradients as high as 150 MV/m, and the viability of accelerating structures capable of achieving this field has been demonstrated in the CLIC test facility [53]. Parameter sets have been calculated for CLIC designs with $E_{\rm CM} = 3, 5$ TeV and luminosities of 10^{35} cm^{-2}s^{-1} or more [51].

In many of the proposed benchmark supersymmetric scenarios, CLIC would be able to complete

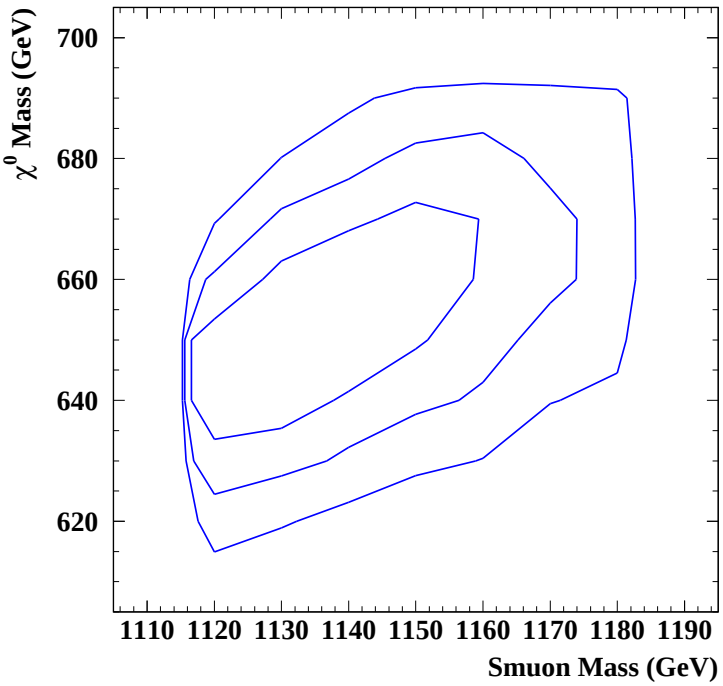

Fig. 12: *Like lower-energy e^+e^- colliders, CLIC enables very accurate measurements of sparticle masses to be made, in this case the supersymmetric partner of the muon and the lightest neutralino χ^0 [54].*

the supersymmetric spectrum and/or measure in much more detail heavy sparticles found previously at the LHC, as seen in Fig. 10 [40]. CLIC produces more beamstrahlung than lower-energy linear e^+e^- colliders, but the supersymmetric missing-energy signature would still be easy to distinguish, and accurate measurements of masses and decay modes could still be made, as seen in Fig. 12 [54].

1.9 Searches for Dark Matter Particles

In the above discussion, we have paid particular attention to the region of parameter space where the lightest supersymmetric particle could constitute the cold dark matter in the Universe [12]. How easy would this be to detect? Fig. 13 shows rates for the elastic spin-independent scattering of supersymmetric relics [55], including the projected sensitivities for CDMS II [56] and CRESST [57] (solid) and GENIUS [58] (dashed). Also shown are the cross sections calculated in the proposed benchmark scenarios discussed in the previous section, which are considerably below the DAMA [59] range ($10^{-5} - 10^{-6}$ pb), but may be within reach of future projects. The prospects for detecting elastic spin-independent scattering are less bright, as also shown in Fig. 13. Indirect searches for supersymmetric dark matter via the products of annihilations in the galactic halo or inside the Sun also have prospects in some of the benchmark scenarios [55], as seen in Fig. 14.

2. Lepton Flavour Violation

2.1 Why not?

There is no good reason why either the total lepton number L or the individual lepton flavours $L_{e,\mu,\tau}$ should be conserved [61]. We have learnt that the only conserved quantum numbers are those associated with exact gauge symmetries, just as the conservation of electromagnetic charge is associated with $U(1)$ gauge invariance. On the other hand, there is no exact gauge symmetry associated with any of the lepton

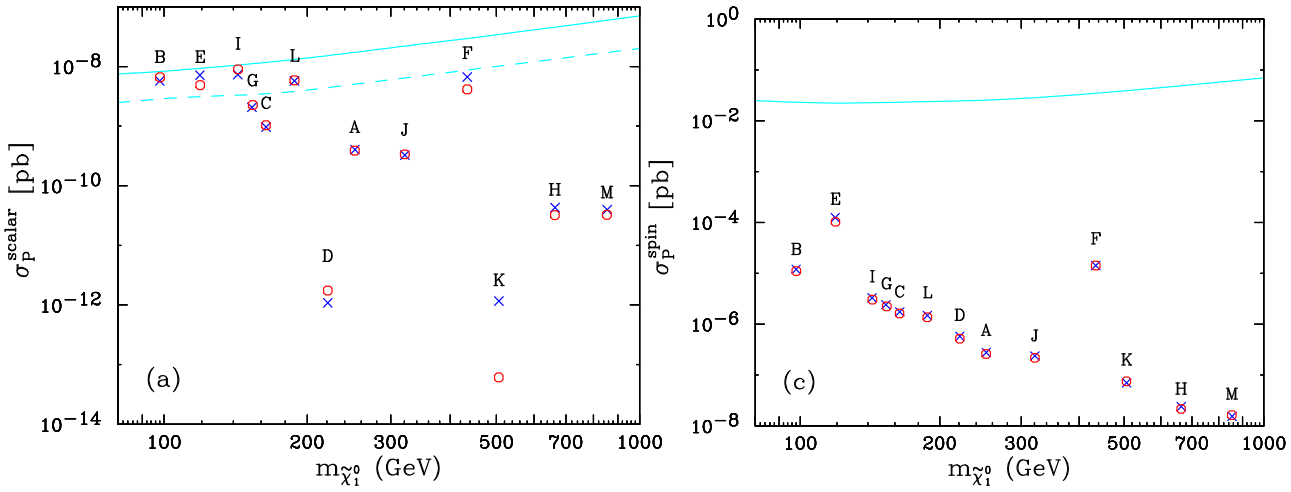

Fig. 13: *Left panel: elastic spin-independent scattering of supersymmetric relics on protons calculated in benchmark scenarios [55], compared with the projected sensitivities for CDMS II [56] and CRESST [57] (solid) and GENIUS [58] (dashed). The predictions of the* `SSARD` *code (blue crosses) and* `Neutdriver`*[60] (red circles) for neutralino-nucleon scattering are compared. The labels A, B, ...,L correspond to the benchmark points as shown in Fig. 6. Right panel: prospects for detecting elastic spin-independent scattering in the benchmark scenarios, which are less bright.*

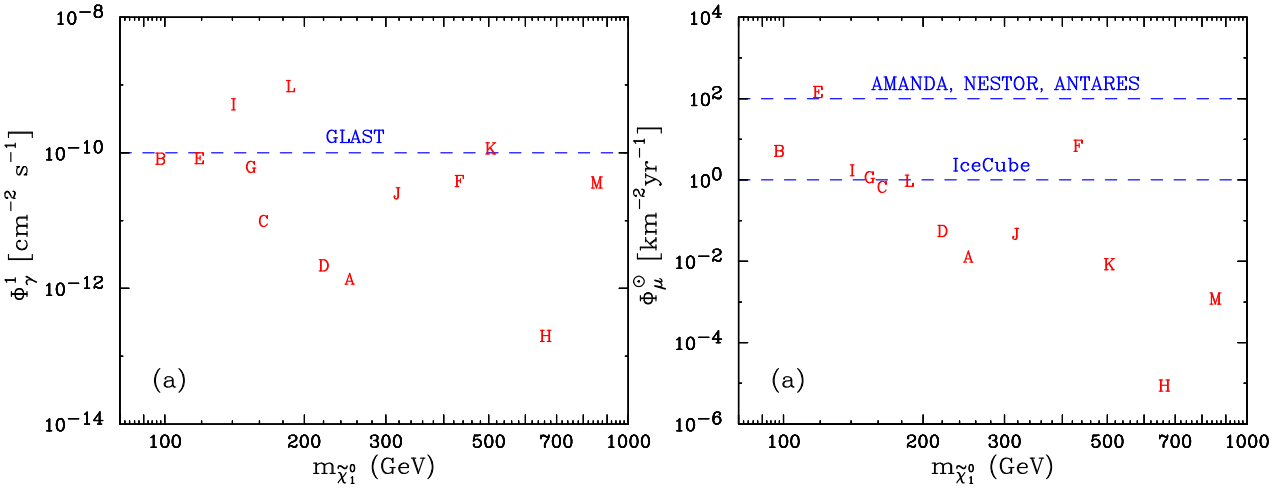

Fig. 14: *Left panel: prospects for detecting photons with energies above 1 GeV from annihilations in the centre of the galaxy, assuming a moderate enhancement there of the overall halo density, and right panel: prospects for detecting muons from energetic solar neutrinos produced by relic annihilations in the Sun, as calculated [55] in the benchmark scenarios using* `Neutdriver`*[60].*

numbers.

Moreover, neutrinos have been seen to oscillate between their different flavours [62, 63], showing that the separate lepton flavours $L_{e,\mu,\tau}$ are indeed not conserved, though the conservation of total lepton number L is still an open question. The observation of such oscillations strongly suggests that the neutrinos have different masses. Again, massless particles are generally associated with exact gauge symmetries, e.g., the photon with the $U(1)$ symmetry of the Standard Model, and the gluons with its $SU(3)$ symmetry. In the absence of any leptonic gauge symmetry, non-zero lepton masses are to be expected, in general.

The conservation of lepton number is an accidental symmetry of the renormalizable terms in the Standard Model lagrangian. However, one could easily add to the Standard Model non-renormalizable terms that would generate neutrino masses, even without introducing a 'right-handed' neutrino field. For example, a non-renormalizable term of the form [64]

$$\frac{1}{M}\nu H \cdot \nu H, \tag{16}$$

where M is some large mass beyond the scale of the Standard Model, would generate a neutrino mass term:

$$m_\nu \nu \cdot \nu : \; m_\nu \; = \; \frac{\langle 0|H|0\rangle^2}{M}. \tag{17}$$

Of course, a non-renormalizable interaction such as (16) seems unlikely to be fundamental, and one should like to understand the origin of the large mass scale M.

The minimal renormalizable model of neutrino masses requires the introduction of weak-singlet 'right-handed' neutrinos N. These will in general couple to the conventional weak-doublet left-handed neutrinos via Yukawa couplings Y_ν that yield Dirac masses $m_D \sim m_W$. In addition, these 'right-handed' neutrinos N can couple to themselves via Majorana masses M that may be $\gg m_W$, since they do not require electroweak summetry breaking. Combining the two types of mass term, one obtains the seesaw mass matrix [65]:

$$(\nu_L, N) \begin{pmatrix} 0 & M_D \\ M_D^T & M \end{pmatrix} \begin{pmatrix} \nu_L \\ N \end{pmatrix}, \tag{18}$$

where each of the entries should be understood as a matrix in generation space.

In order to provide the two measured differences in neutrino masses-squared, there must be at least two non-zero masses, and hence at least two heavy singlet neutrinos N_i [66, 67]. Presumably, all three light neutrino masses are non-zero, in which case there must be at least three N_i. This is indeed what happens in simple GUT models such as SO(10), but some models [68] have more singlet neutrinos [69]. In this Lecture, for simplicity we consider just three N_i.

As we discuss in the next Section, this seesaw model can accommodate the neutrino mixing seen experimentally, and naturally explains the small differences in the masses-squared of the light neutrinos. By itself, it would lead to unobservably small transitions between the different charged-lepton flavours. However, supersymmetry may enhance greatly the rates for processes violating the different charged-lepton flavours, rendering them potentially observable, as we discuss in subsequent Sections.

2.2 Neutrino Masses and Mixing in the Seesaw Model

The effective mass matrix for light neutrinos in the seesaw model may be written as:

$$\mathcal{M}_\nu \; = \; Y_\nu^T \frac{1}{M} Y_\nu v^2 \left[\sin^2\beta\right] \tag{19}$$

where we have used the relation $m_D = Y_\nu v \left[\sin\beta\right]$ with $v \equiv \langle 0|H|0\rangle$, and the factors of $\sin\beta$ appear in the supersymmetric version of the seesaw model. It is convenient to work in the field basis where the

charged-lepton masses $m_{\ell^\pm}$ and the heavy singlet-neutrino mases M are real and diagonal. The seesaw neutrino mass matrix $\mathcal{M}_\nu$ (19) may then be diagonalized by a unitary transformation U:

$$U^T \mathcal{M}_\nu U \; = \; \mathcal{M}_\nu^d. \tag{20}$$

This diagonalization is reminiscent of that required for the quark mass matrices in the Standard Model. In that case, it is well known that one can redefine the phases of the quark fields [70] so that the mixing matrix U_{CKM} has just one CP-violating phase [71]. However, in the neutrino case, there are fewer independent field phases, and one is left with three physical CP-violating parameters:

$$U \; = \; \tilde{P}_2 V P_0 : \; P_0 \equiv \mathrm{Diag}\left(e^{i\phi_1}, e^{i\phi_2}, 1\right). \tag{21}$$

Here $\tilde{P}_2 = \mathrm{Diag}\left(e^{i\alpha_1}, e^{i\alpha_2}, e^{i\alpha_3}\right)$ contains three phases that can be removed by phase rotations and are unobservable in light-neutrino physics, V is the light-neutrino mixing matrix first considered by Maki, Nakagawa and Sakata (MNS) [72], and P_0 contains 2 observable CP-violating phases $\phi_{1,2}$. The MNS matrix describes neutrino oscillations

$$V \; = \; \begin{pmatrix} c_{12} & s_{12} & 0 \\ -s_{12} & c_{12} & 0 \\ 0 & 0 & 1 \end{pmatrix} \begin{pmatrix} 1 & 0 & 0 \\ 0 & c_{23} & s_{23} \\ 0 & -s_{23} & c_{23} \end{pmatrix} \begin{pmatrix} c_{13} & 0 & s_{13} \\ 0 & 1 & 0 \\ -s_{13}e^{-i\delta} & 0 & c_{13}e^{-i\delta} \end{pmatrix}. \tag{22}$$

The Majorana phases $\phi_{1,2}$ are in principle observable in neutrinoless double-β decay, whose matrix element is proportional to

$$\langle m_\nu \rangle_{ee} \; \equiv \; \Sigma_i U_{ei}^* m_{\nu_i} U_{ie}^\dagger. \tag{23}$$

Later we discuss how other observable quantities might be sensitive indirectly to the Majorana phases.

The first matrix factor in (22) is measurable in solar neutrino experiments. As seen in Fig. 15, the recent data from SNO [63] and Super-Kamiokande [73] prefer quite strongly the large-mixing-angle (LMA) solution to the solar neutrino problem with $\Delta m^2_{12} \sim 6 \times 10^{-5}$ eV^2, though the LOW solution with lower δm^2 cannot yet be ruled out. The data favour large but non-maximal mixing: $\theta_{12} \sim 30^o$. The second matrix factor in (22) is measurable in atmospheric neutrino experiments. As seen in Fig. 16, the data from Super-Kamiokande in particular [62] favour maximal mixing of atmospheric neutrinos: $\theta_{23} \sim 45^o$ and $\Delta m^2_{23} \sim 2.5 \times 10^{-3}$ eV^2. The third matrix factor in (22) is basically unknown, with experiments such as Chooz [74] and Super-Kamiokande only establishing upper limits on θ_{13}, and *a fortiori* no information on the CP-violating phase δ.

The phase δ could in principle be measured by comparing the oscillation probabilities for neutrinos and antineutrinos and computing the CP-violating asymmetry [75]:

$$\begin{aligned} P\left(\nu_e \to \nu_\mu\right) - P\left(\bar{\nu}_e \to \bar{\nu}_\mu\right) \quad &= \; 16 s_{12} c_{12} s_{13} c_{13}^2 s_{23} c_{23} \sin\delta \\ &\sin\left(\frac{\Delta m^2_{12}}{4E} L\right) \sin\left(\frac{\Delta m^2_{13}}{4E} L\right) \sin\left(\frac{\Delta m^2_{23}}{4E} L\right), \end{aligned} \tag{24}$$

as seen in Fig. 17 [76, 77]. This is possible only if Δm^2_{12} and s_{12} are large enough - as now suggested by the success of the LMA solution to the solar neutrino problem, and if s_{13} is large enough - which remains an open question.

We have seen above that the effective low-energy mass matrix for the light neutrinos contains 9 parameters, 3 mass eigenvalues, 3 real mixing angles and 3 CP-violating phases. However, these are not all the parameters in the minimal seesaw model. As shown in Fig. 18, this model has a total of 18 parameters [78, 2]. Most of the rest of this Lecture is devoted to understanding better the origins and possible manifestations of the remaining parameters, many of which may have controlled the generation of matter in the Universe via leptogenesis [79] and may be observable via renormalization in supersymmetric models [80, 2, 81, 82].

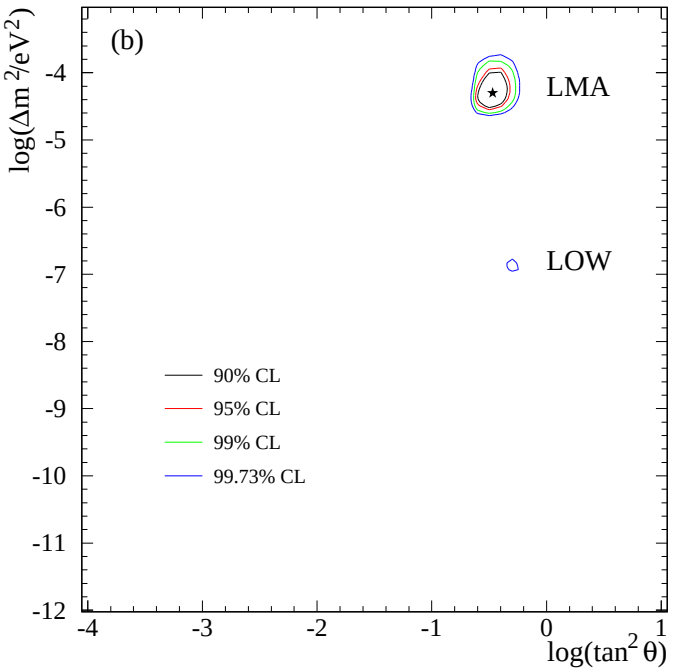

Fig. 15: *A global fit to solar neutrino data, following the SNO measurements of the total neutral-current reaction rate, the energy spectrum and the day-night asymmetry, favours large mixing and* $\Delta m^2 \sim 6 \times 10^{-5}$ *eV*^{2} *[63].*

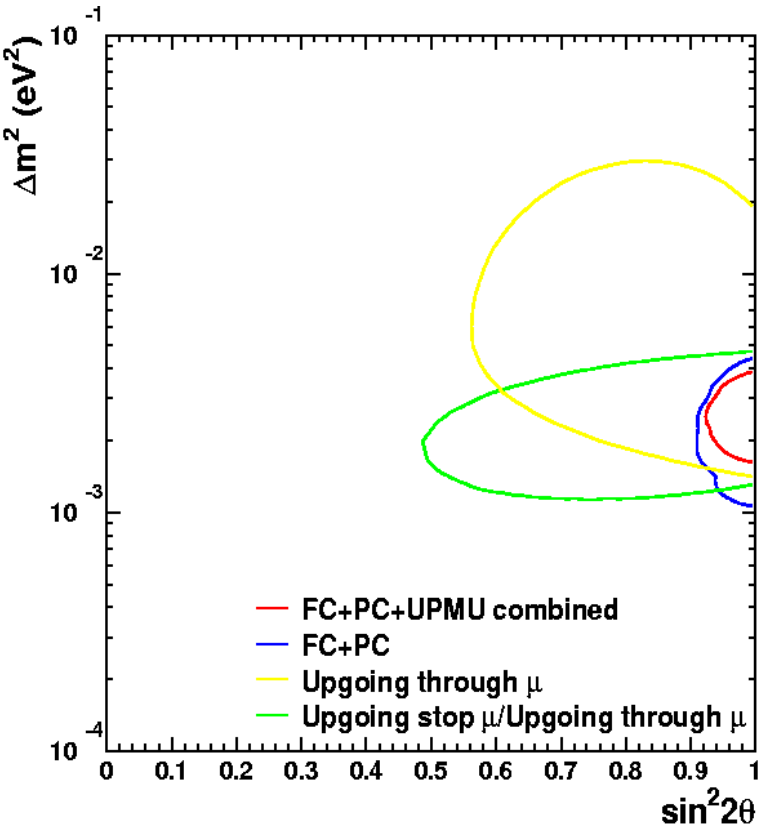

Fig. 16: *A fit to the Super-Kamiokande data on atmospheric neutrinos [62] indicates near-maximal* $\nu_\mu - \nu_\tau$ *mixing with* $\Delta m^2 \sim 2.5 \times 10^{-3}$ *eV*^{2}.

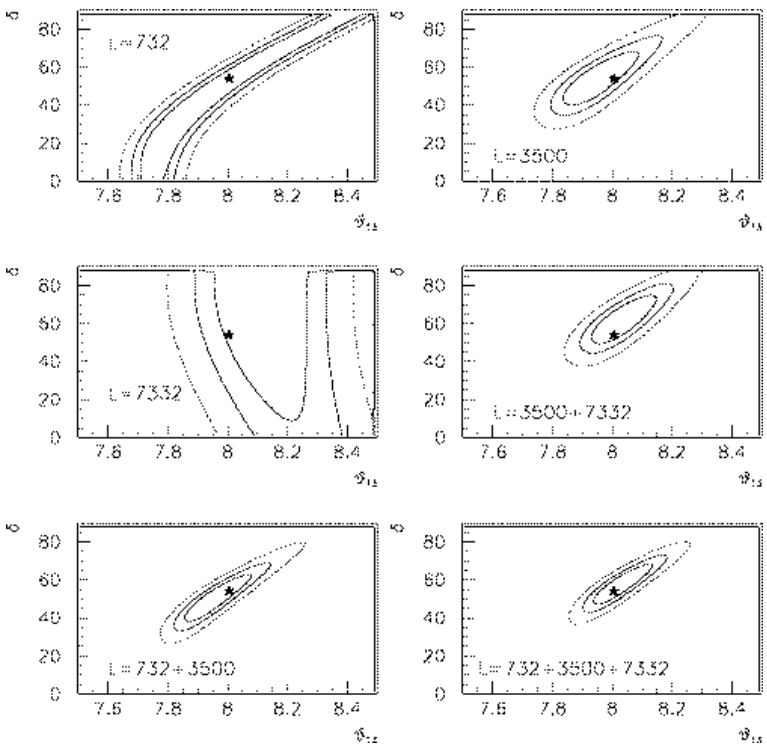

Fig. 17: *Correlations in a simultaneous fit of θ_{13} and δ, using a neutrino energy threshold of about 10 GeV. Using a single baseline correlations are very strong, but can be largely reduced by combining information from different baselines and detector techniques [76], enabling the CP-violating phase δ to be extracted.*

To see how the extra 9 parameters appear [2], we reconsider the full lepton sector, assuming that we have diagonalized the charged-lepton mass matrix:

$$(Y_\ell)_{ij} \;=\; Y^d_{\ell_i}\delta_{ij}, \tag{25}$$

as well as that of the heavy singlet neutrinos:

$$M_{ij} \;= M^d_i\delta_{ij}. \tag{26}$$

We can then parametrize the neutrino Dirac coupling matrix Y_ν in terms of its real and diagonal eigenvalues and unitary rotation matrices:

$$Y_\nu \;=\; Z^* Y^d_{\nu_k} X^\dagger, \tag{27}$$

where X has 3 mixing angles and one CP-violating phase, just like the CKM matrix, and we can write Z in the form

$$Z \;=\; P_1 \bar{Z} P_2, \tag{28}$$

where $\bar{Z}$ also resembles the CKM matrix, with 3 mixing angles and one CP-violating phase, and the diagonal matrices $P_{1,2}$ each have two CP-violating phases:

$$P_{1,2} \;=\; \mathrm{Diag}\left(e^{i\theta_{1,3}}, e^{i\theta_{2,4}}, 1\right). \tag{29}$$

In this parametrization, we see explicitly that the neutrino sector has 18 parameters: the 3 heavy-neutrino mass eigenvalues M^d_i, the 3 real eigenvalues of $Y^D_{\nu_i}$, the $6 = 3 + 3$ real mixing angles in X and $\bar{Z}$, and the $6 = 1 + 5$ CP-violating phases in X and $\bar{Z}$ [2].

As we discuss later in more detail, leptogenesis [79] is proportional to the product

$$Y_\nu Y_\nu^\dagger \;=\; P_1^* \bar{Z}^* \left(Y^d_\nu\right)^2 \bar{Z}^T P_1, \tag{30}$$

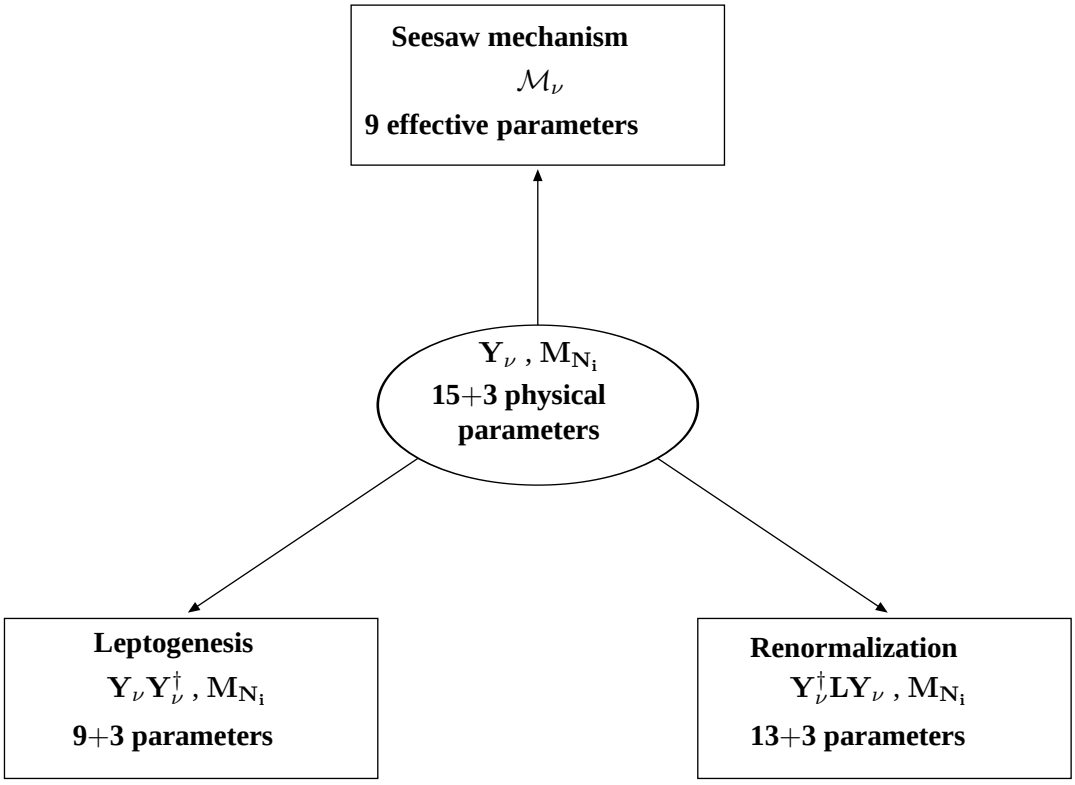

Fig. 18: *Roadmap for the physical observables derived from Y_ν and N_i [83].*

which depends on 13 of the real parameters and 3 CP-violating phases, whilst the leading renormalization of soft supersymmetry-breaking masses depends on the combination

$$Y_\nu^\dagger Y_\nu \; = \; X \left(Y_\nu^d\right)^2 X^\dagger, \tag{31}$$

which depends on just 1 CP-violating phase, with two more phases appearing in higher orders, when one allows the heavy singlet neutrinos to be non-degenerate [81].

In order to see how the low-energy sector is embedded in this full parametrization, we first recall that the 3 phases in $\tilde{P}_2$ (21) become observable when one also considers high-energy quantities. Next, we introduce a complex orthogonal matrix

$$R \; \equiv \; \sqrt{M^d}^{-1} Y_\nu U \sqrt{M^d}^{-1} \left[v \sin\beta\right], \tag{32}$$

which has 3 real mixing angles and 3 phases: $R^T R = 1$. These 6 additional parameters may be used to characterize Y_ν, by inverting (32):

$$Y_\nu \; = \; \frac{\sqrt{M^d} R \sqrt{M^d} U^\dagger}{\left[v \sin\beta\right]}, \tag{33}$$

giving us the same grand total of $18 = 9 + 3 + 6$ parameters [2]. The leptogenesis observable (30) may now be written in the form

$$Y_\nu Y_\nu^\dagger \; = \; \frac{\sqrt{M^d} R \mathcal{M}_\nu^d R^\dagger \sqrt{M^d}}{\left[v^2 \sin^2\beta\right]}, \tag{34}$$

which depends on the 3 phases in R, but *not* the 3 low-energy phases $\delta, \phi_{1,2}$, *nor* the 3 real MNS mixing

angles [2]! Conversely, the leading renormalization observable (31) may be written in the form

$$Y_\nu^\dagger Y_\nu \; = \; U \frac{\sqrt{\mathcal{M}_\nu^d} R^\dagger M^d R \sqrt{\mathcal{M}_\nu^d}}{\left[v^2 \sin^2\beta\right]} U^\dagger, \tag{35}$$

which depends explicitly on the MNS matrix, including the CP-violating phases δ and $\phi_{1,2}$, but only one of the three phases in $\tilde{P}_2$ [2].

2.3 Renormalization of Soft Supersymmetry-Breaking Parameters

Let us now discuss the renormalization of soft supersymmetry-breaking parameters m_0^2 and A in more detail, assuming that the input values at the GUT scale are flavour-independent. If they are not, there will be additional sources of flavour-changing processes, beyond those discussed in this and subsequent sections [14, 84]. In the leading-logarithmic approximation, and assuming degenerate heavy singlet neutrinos, one finds the following radiative corrections to the soft supersymmetry-breaking terms for sleptons:

$$\begin{aligned} \left(\delta m_{\tilde{L}}^2\right)_{ij} &= -\frac{1}{8\pi^2}\left(3m_0^2 + A_0^2\right)\left(Y_\nu^\dagger Y_\nu\right)_{ij} \mathrm{Ln}\left(\frac{M_{GUT}}{M}\right), \\ (\delta A_\ell)_{ij} &= -\frac{1}{8\pi^2} A_0 Y_{\ell_i}\left(Y_\nu^\dagger Y_\nu\right)_{ij} \mathrm{Ln}\left(\frac{M_{GUT}}{M}\right), \end{aligned} \tag{36}$$

where we have intially assumed that the heavy singlet neutrinos are approximately degenerate with $M \ll M_{GUT}$. In this case, there is a single analogue of the Jarlskog invariant of the Standard Model [85]:

$$J_{\tilde{L}} \; \equiv \; \mathrm{Im}\left[\left(m_{\tilde{L}}^2\right)_{12}\left(m_{\tilde{L}}^2\right)_{23}\left(m_{\tilde{L}}^2\right)_{31}\right], \tag{37}$$

which depends on the single phase that is observable in this approximation. There are other Jarlskog invariants defined analogously in terms of various combinations with the A_ℓ, but these are all proportional [2].

There are additional contributions if the heavy singlet neutrinos are not degenerate:

$$\left(\tilde{\delta} m_{\tilde{L}}^2\right)_{ij} \; = \; -\frac{1}{8\pi^2}\left(3m_0^2 + A_0^2\right)\left(Y_\nu^\dagger L Y_\nu\right)_{ij} : \; L \equiv \mathrm{Ln}\left(\frac{\bar{M}}{M_i}\right)\delta_{ij}, \tag{38}$$

where $\bar{M} \equiv \sqrt[3]{M_1 M_2 M_3}$, with $\left(\tilde{\delta} A_\ell\right)_{ij}$ being defined analogously. These new contributions contain the matrix factor

$$Y^\dagger L Y \; = \; X Y^d P_2 \bar{Z}^T L \bar{Z}^* P_2^* y^d X^\dagger, \tag{39}$$

which introduces dependences on the phases in $\bar{Z}P_2$, though not P_1. In this way, the renormalization of the soft supersymmetry-breaking parameters becomes sensitive to a total of 3 CP-violating phases [81].

2.4 Exploration of Parameter Space

Now that we have seen how the 18 parameters in the minimal supersymmetric seesaw model might in principle be observable, we would like to explore the range of possibilities in this parameter space. This requires confronting two issues: the unwieldy large dimensionality of the parameter space, and the inclusion of the experimental information already obtained (or obtainable) from low-energy studies of neutrinos. Of the 9 parameters accessible to these experiments: $m_{\nu_1}, m_{\nu_2}, m_{\nu_3}, \theta_{12}, \theta_{23}, \theta_{31}, \delta, \phi_1$ and ϕ_2, we have measurements of 4 combinations: $\Delta m_{12}^2, \Delta m_{23}^2, \theta_{12}$ and θ_{23}, and upper limits on the overall light-neutrino mass scale, θ_{13} and the double-β decay observable (23).

The remaining 9 parameters not measurable in low-energy neutrino physics may be characterized by an auxiliary Hermitean matrix of the following form [80, 82]:

$$H \equiv Y_\nu^\dagger D Y_\nu, \tag{40}$$

where D is an arbitrary real and diagonal matrix. Possible choices for D include $\mathrm{Diag}(\pm 1, \pm 1, \pm 1)$ and the logarithmic matrix L defined in (38). Once one specifies the 9 parameters in H, either in a statistical survey or in some definite model, one can calculate

$$H' \equiv \sqrt{\mathcal{M}_\nu^d} U^\dagger H U \sqrt{\mathcal{M}_\nu^d}, \tag{41}$$

which can then be diagonalized by a complex orthogonal matrix R':

$$H' = R'^\dagger \mathcal{M}'^d R' : \; R'^T R' = 1. \tag{42}$$

In this way, we can calculate all the remaining physical parameters:

$$(\mathcal{M}_\nu, H) \to (\mathcal{M}_\nu, \mathcal{M}'^d, R') \to (Y_\nu, M_i) \tag{43}$$

and then go on to calculate leptogenesis, charged-lepton violation, etc [80, 82].

A freely chosen model will in general violate the experimental upper limit on $\mu \to e\gamma$ [86]. It is easy to avoid this problem using the parametrization (40) [82]. If one chooses $D = L$ and requires the entry $H_{12} = 0$, the leading contribution to $\mu \to e\gamma$ from renormalization of the soft supersymmetry-breaking masses will be suppressed. To suppress $\mu \to e\gamma$ still further, one may impose the constraint $H_{13}H_{23} = 0$. This condition evidently has two solutions: either $H_{13} = 0$, in which case $\tau \to e\gamma$ is suppressed but not $\tau \to \mu\gamma$, or alternatively $H_{23} = 0$, which favours $\tau \to e\gamma$ over $\tau \to \mu\gamma$. Thus we may define two generic textures H^1 and H^2:

$$H^1 \equiv \begin{pmatrix} a & 0 & 0 \\ 0 & b & d \\ 0 & d^\dagger & c \end{pmatrix}, \; H^2 \equiv \begin{pmatrix} a & 0 & d \\ 0 & b & 0 \\ d^\dagger & 0 & c \end{pmatrix}. \tag{44}$$

We use these as guides in the following, whilst recalling that they represent extremes, and the truth may not favour one $\tau \to \ell\gamma$ decay mode so strongly over the other.

2.5 Leptogenesis

In addition to the low-energy neutrino constraints, we frequently employ the constraint that the model parameters be compatible with the leptogenesis scenario for creating the baryon asymmetry of the Universe [79]. We recall that the baryon-to-entropy ratio Y_B in the Universe today is found to be in the range $10^{-11} < Y_B < 3 \times 10^{-10}$. This is believed to have evolved from a similar asymmetry in the relative abundances of quarks and antiquarks before they became confined inside hadrons when the temperature of the Universe was about 100 MeV. In the leptogenesis scenario [79], non-perturbative electroweak interactions caused this small asymmetry to evolve out of a similar small asymmetry in the relative abundances of leptons and antileptons that had been generated by CP violation in the decays of heavy singlet neutrinos.

The total decay rate of such a heavy neutrino N_i may be written in the form

$$\Gamma_i = \frac{1}{8\pi} \left(Y_\nu Y_\nu^\dagger \right)_{ii} M_i. \tag{45}$$

One-loop CP-violating diagrams involving the exchange of heavy neutrino N_j would generate an asymmetry in N_i decay of the form:

$$\epsilon_{ij} = \frac{1}{8\pi} \frac{1}{\left(Y_\nu Y_\nu^\dagger \right)_{ii}} \mathrm{Im} \left(\left(Y_\nu Y_\nu^\dagger \right)_{ij} \right)^2 f\left(\frac{M_j}{M_i} \right), \tag{46}$$

where $f(M_j/M_i)$ is a known kinematic function.

As already remarked, the relevant combination

$$\left(Y_\nu Y_\nu^\dagger\right) \; = \; \sqrt{M^d} R \mathcal{M}^d R^\dagger \sqrt{M^d} \tag{47}$$

is independent of U and hence of the light neutrino mixing angles and CP-violating phases. The basic reason for this is that one makes a unitary sum over all the light lepton species in evaluating the asymmetry ϵ_{ij}. It is easy to derive a compact expression for ϵ_{ij} in terms of the heavy neutrino masses and the complex orthogonal matrix R:

$$\epsilon_{ij} \; = \; \frac{1}{8\pi} M_j f\left(\frac{M_j}{M_i}\right) \frac{{\rm Im}\left(\left(R\mathcal{M}_\nu^d R^\dagger\right)_{ij}\right)^2}{\left(R\mathcal{M}_\nu^d R^\dagger\right)_{ii}}. \tag{48}$$

This depends explicitly on the extra phases in R: how can we measure them?

The basic principle of a strategy to do this is the following [2, 81, 82]. The renormalization of soft supersymmetry-breaking parameters, and hence flavour-changing interactions and CP violation in the lepton sector, depend on the leptogenesis parameters as well as the low-energy neutrino parameters $\delta, \phi_{1,2}$. If one measures the latter in neutrino experiments, and the discrepancy in the soft supersymmetry-breaking determines the leptogenesis parameters.

An example how this could work is provided by the two-generation version of the supersymmetric seesaw model [2]. In this case, we have $\mathcal{M}_\nu^d = {\rm Diag}(m_{\nu_1}, m_{\nu_1})$ and $M^d = {\rm Diag}(M_1, M_2)$, and we may parameterize

$$R \; = \; \begin{pmatrix} \cos(\theta_r + i\theta_i) & \sin(\theta_r + i\theta_i) \\ -\sin(\theta_r + i\theta_i) & \cos(\theta_r + i\theta_i) \end{pmatrix}. \tag{49}$$

In this case, the leptogenesis decay asymmetry is proportional to

$${\rm Im}\left(\left(Y_\nu Y_\nu^\dagger\right)^{21}\right)^2 \; = \; \frac{\left(m_{\nu_1}^2 - m_{\nu_2}^2\right) M_1 M_2}{2v^4 \sin^4\beta} {\rm sinh}2\theta_i sin2\theta_r. \tag{50}$$

We see that this is related explicitly to the CP-violating phase and mixing angle in R (49), and is independent of the low-energy neutrino parameters. Turning now to the renormalization of the soft supersymmetry-breaking parameters, assuming for simplicity maximal mixing in the MNS matrix V and setting the diagonal Majorana phase matrix $P_0 = {\rm Diag}(e^{-i\phi}, 1)$, we find that

$$\begin{aligned} {\rm Re}\left[\left(Y_\nu^\dagger Y_\nu\right)^{12}\right] \; &= \; -\frac{\left(m_{\nu_2} - m_{\nu_1}\right)}{4v^2 \sin^2\beta}(M_1 + M_2){\rm cosh}2\theta_i \; + \; \cdots, \\ {\rm Im}\left[\left(Y_\nu^\dagger Y_\nu\right)^{12}\right] \; &= \; \frac{\sqrt{m_{\nu_2} m_{\nu_1}}}{2v^2 \sin^2\beta}(M_1 + M_2){\rm sinh}2\theta_i \cos\phi \; + \; \cdots. \end{aligned} \tag{51}$$

In this case, the strategy for relating leptogenesis to low-energy observables would be: (i) use double-β decay to determine ϕ, (ii) use low-energy observables sensitive to ${\rm Re}, {\rm Im}\left[\left(Y_\nu^\dagger Y_\nu\right)^{12}\right]$ to determine θ_r and θ_i (51), which then (iii) determine the leptogenesis asymmetry (50) in this two-generation model.

In general, one may formulate the following strategy for calculating leptogenesis in terms of laboratory observables:

- Measure the neutrino oscillation phase δ and the Majorana phases $\phi_{1,2}$,
- Measure observables related to the renormalization of soft supersymmetry-breaking parameters, that are functions of $\delta, \phi_{1,2}$ and the leptogenesis phases,
- Extract the effects of the known values of δ and $\phi_{1,2}$, and isolate the leptogenesis parameters.

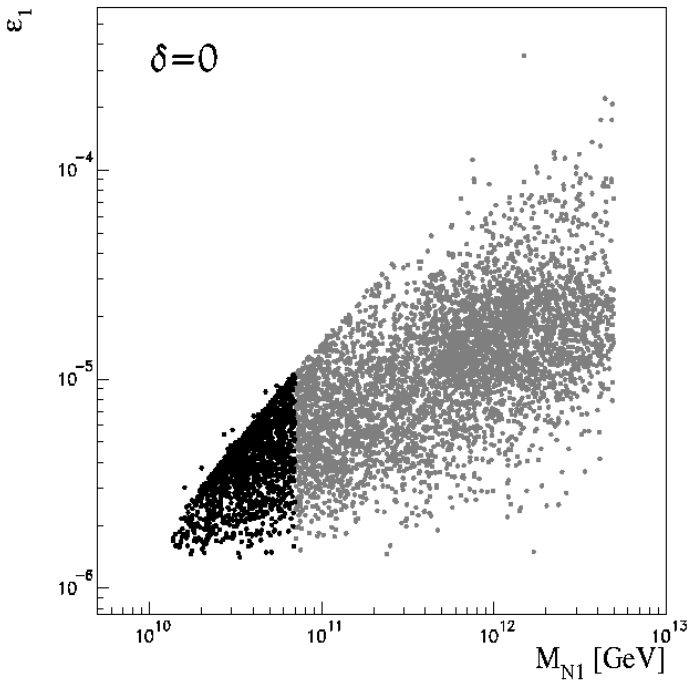

Fig. 19: *Heavy singlet neutrino decay may exhibit a CP-violating asymmetry, leading to leptogenesis and hence baryogenesis, even if the neutrino oscillation phase δ vanishes [83].*

In the absence of complete information on the first two steps above, we are currently at the stage of preliminary explorations of the multi-dimensional parameter space. As seen in Fig. 19, the amount of the leptogenesis asymmetry is explicitly independent of δ [83]. An important observation is that there is a non-trivial lower bound on the mass of the lightest heavy singlet neutrino N:

$$M_{N_1} \gtrsim 10^{10}\ \mathrm{GeV} \tag{52}$$

if the light neutrinos have the conventional hierarchy of masses, and

$$M_{N_1} \gtrsim 10^{11}\ \mathrm{GeV} \tag{53}$$

if they have an inverted hierarchy of masses [83]. This observation is potentially important for the cosmological abundance of gravitinos, which would be problematic if the cosmological temperature was once high enough for leptogenesis by thermally-produced singlet neutrinos weighing as much as (52, 53) [87]. However, these bounds could be relaxed if the two lightest N_i were near-degenerate, as seen in Fig. 20 [88]. Striking aspects of this scenario include the suppression of $\mu \to e\gamma$, the relatively large value of $\tau \to \mu\gamma$, and a preferred value for the neutrinoless double-β decay observable:

$$\langle m \rangle_{ee} \sim \sqrt{\Delta m^2_{solar}}\, \sin^2 \theta_{12}. \tag{54}$$

2.6 Flavour-Violating Decays of Charged Leptons

Several such decays can be studied within this framework, including $\mu \to e\gamma, \tau \to e\gamma, \tau \to \mu\gamma, \mu \to 3e$, and $\tau \to 3\mu/e$ [89].

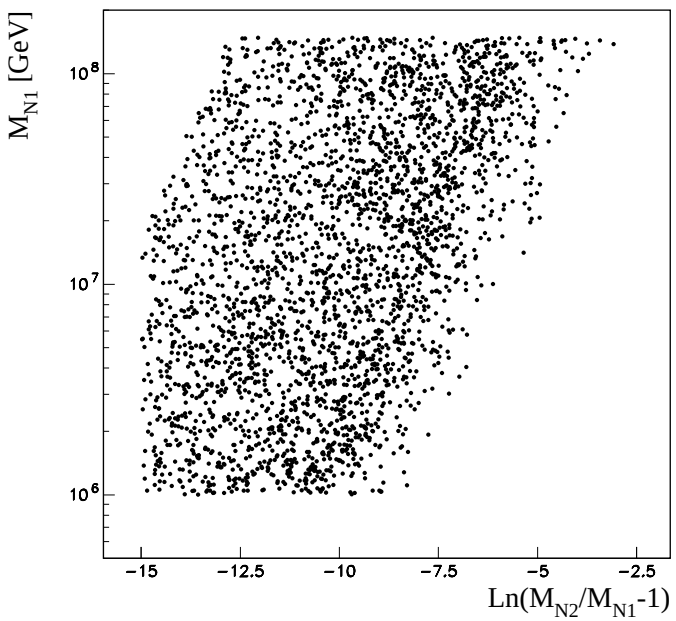

Fig. 20: *The lower limit on the mass of the lightest heavy singlet neutrino may be significantly reduced if the two lightest singlet neutrinos are almost degenerate [88].*

The effective Lagrangian for $\mu \to e\gamma$ and $\mu \to 3e$ can be written in the form [90, 2]:

$$\begin{aligned}\mathcal{L} \;=\; & -\frac{4G_F}{\sqrt{2}}\{m_\mu A_R \overline{\mu_R}\sigma^{\mu\nu} e_L F_{\mu\nu} + m_\mu A_L \overline{\mu_L}\sigma^{\mu\nu} e_R F_{\mu\nu} \\ & + g_1(\overline{\mu_R}e_L)(\overline{e_R}e_L) + g_2(\overline{\mu_L}e_R)(\overline{e_L}e_R) \\ & + g_3(\overline{\mu_R}\gamma^\mu e_R)(\overline{e_R}\gamma_\mu e_R) + g_4(\overline{\mu_L}\gamma^\mu e_L)(\overline{e_L}\gamma_\mu e_L) \\ & + g_5(\overline{\mu_R}\gamma^\mu e_R)(\overline{e_L}\gamma_\mu e_L) + g_6(\overline{\mu_L}\gamma^\mu e_L)(\overline{e_R}\gamma_\mu e_R) + h.c.\}. \end{aligned} \tag{55}$$

The decay $\mu \to e\gamma$ is related directly to the coefficients $A_{L,R}$:

$$Br(\mu^+ \to e^+\gamma) = 384\pi^2 \left(|A_L|^2 + |A_R|^2\right), \tag{56}$$

and the branching ratio for $\mu \to 3e$ is given by

$$B(\mu \to e\gamma) \;=\; 2(C_1{+}C_2){+}C_3{+}C_4{+}32\left(\ln\frac{m_\mu^2}{m_e^2} - \frac{11}{4}\right)(C_5{+}C_6){+}16(C_7{+}C_8){+}8(C_9{+}C_{10}), \tag{57}$$

where

$$\begin{aligned} & C_1 = \frac{|g_1|^2}{16} + |g_3|^2,\; C_2 = \frac{|g_2|^2}{16} + |g_4|^2, \\ & C_3 = |g_5|^2,\; C_4 = |g_6|^2, C_5 = |eA_R|^2,\; C_6 = |eA_L|^2,\; C_7 = \mathrm{Re}(eA_R g_4^*), \\ & C_8 = \mathrm{Re}(eA_L g_3^*),\; C_9 = \mathrm{Re}(eA_R g_6^*),\; C_{10} = \mathrm{Re}(eA_L g_5^*)\,.. \end{aligned} \tag{58}$$

These coefficients may easily be calculated using the renormalization-group equations for soft supersymmetry-breaking parameters [2, 82].

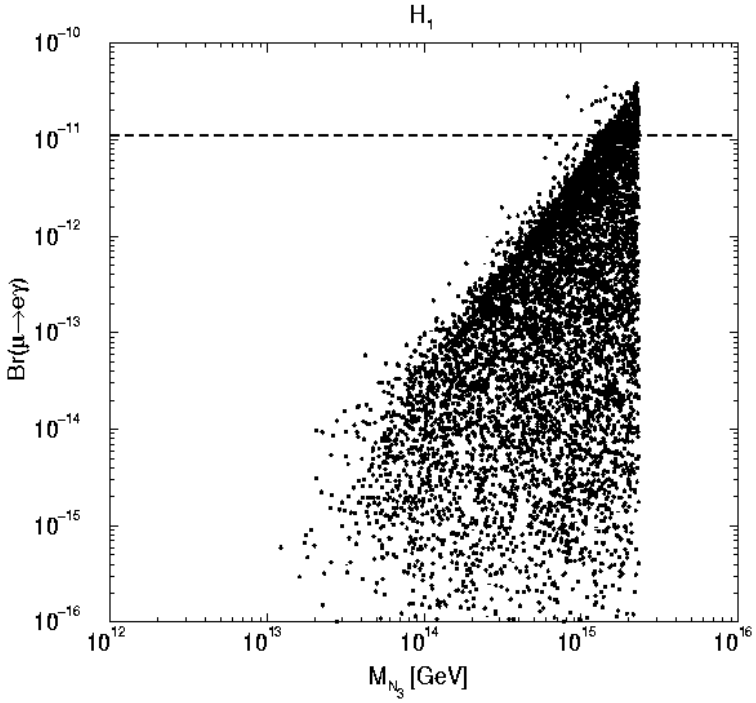

Fig. 21: *Scatter plot of the branching ratio for $\mu \to e\gamma$ in the supersymmetric seesaw model for various values of its unknown parameters [82].*

Fig. 21 displays a scatter plot of $B(\mu \to e\gamma)$ in the texture H^1 mentioned earlier, as a function of the singlet neutrino mass M_{N_3}. We see that $\mu \to e\gamma$ may well have a branching ratio close to the present experimental upper limit, particularly for larger M_{N_3}. Predictions for $\tau \to \mu\gamma$ and $\tau \to e\gamma$ decays are shown in Figs. 22 and 23 for the textures H^1 and H^2, respectively. As advertized earlier, the H^1 texture favours $\tau \to \mu\gamma$ and the H^2 texture favours $\tau \to e\gamma$. We see that the branching ratios decrease with increasing sparticle masses, but that the range due to variations in the neutrino parameters is considerably larger than that due to the sparticle masses. The present experimental upper limits on $\tau \to \mu\gamma$, in particular, already exclude significant numbers of parameter choices.

The branching ratio for $\mu \to 3e$ is usually dominated by the photonic penguin diagram, which contributes the $C_{5,6}$ terms in (57), yielding an essentially constant ratio for $B(\mu \to 3e)/B(\mu \to e\gamma)$. However, if $\mu \to e\gamma$ decay is parametrically suppressed, as it may have to be in order to respect the experimental upper bound on this decay, then other diagrams may become important in $\mu \to 3e$ decay. In this case, the ratio $B(\mu \to 3e)/B(\mu \to e\gamma)$ may be enhanced, as seen in Fig. 24.

As a result, interference between the photonic penguin diagram and the other diagrams may in principle generate a measurable T-odd asymmetry in $\mu \to 3e$ decay. This is sensitive to the CP-violating parameters in the supersymmetric seesaw model, and is in principle observable in polarized $\mu^+ \to e^+e^-e^+$ decay:

$$A_T(\mu^+ \to e^+e^-e^+) = \frac{3}{2\mathcal{B}}\left(2.0C_{11} - 1.6C_{12}\right), \tag{59}$$

where

$$C_{11} = \mathrm{Im}\left(eA_R g_4^* + eA_L g_3^*\right), C_{12} = \mathrm{Im}\left(eA_R g_6^* + eA_L g_5^*\right), \tag{60}$$

and $\mathcal{B}$ is the $\mu \to 3e$ branching ratio with an optimized cutoff for the more energetic positron:

$$\mathcal{B} = 1.8(C_1 + C_2) + 0.96(C_3 + C_4) + 88(C_5 + C_6) + 14(C_7 + C_8) + 8(C_9 + C_{10}). \tag{61}$$

As seen in Fig. 25, the T-odd asymmetry is enhanced in regions of parameter space where $B(\mu \to e\gamma)$

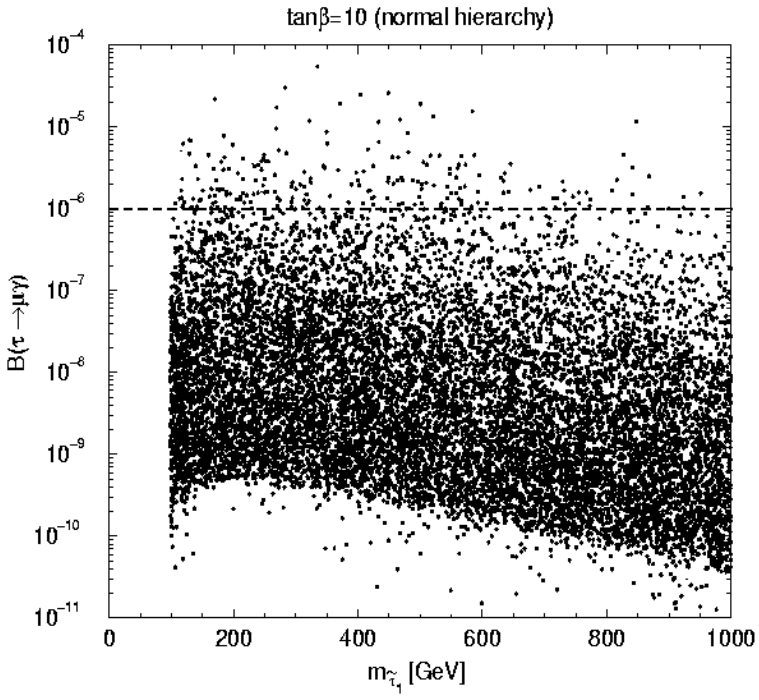

Fig. 22: *Scatter plot of the branching ratio for $\tau \to \mu\gamma$ in one variant of the supersymmetric seesaw model for various values of its unknown parameters [82].*

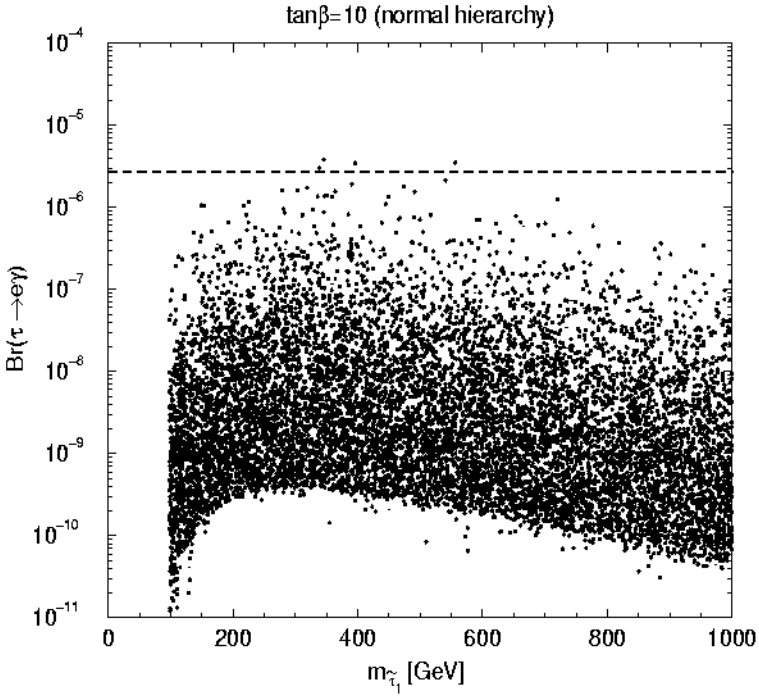

Fig. 23: *Scatter plot of the branching ratio for $\tau \to e\gamma$ in a variant the supersymmetric seesaw model for various values of its unknown parameters [82].*

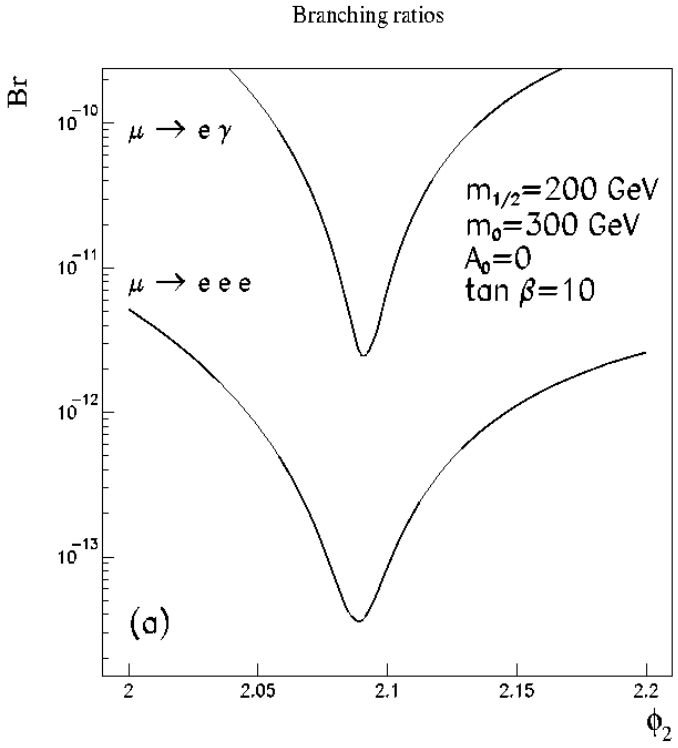

Fig. 24: *The branching ratio for $\mu \rightarrow e\gamma$ may be suppressed for some particular values of the model parameters, in which case the branching ratio for $\mu \rightarrow 3e$ gets significant contributions form other diagrams besides the photonic penguin diagram [2].*

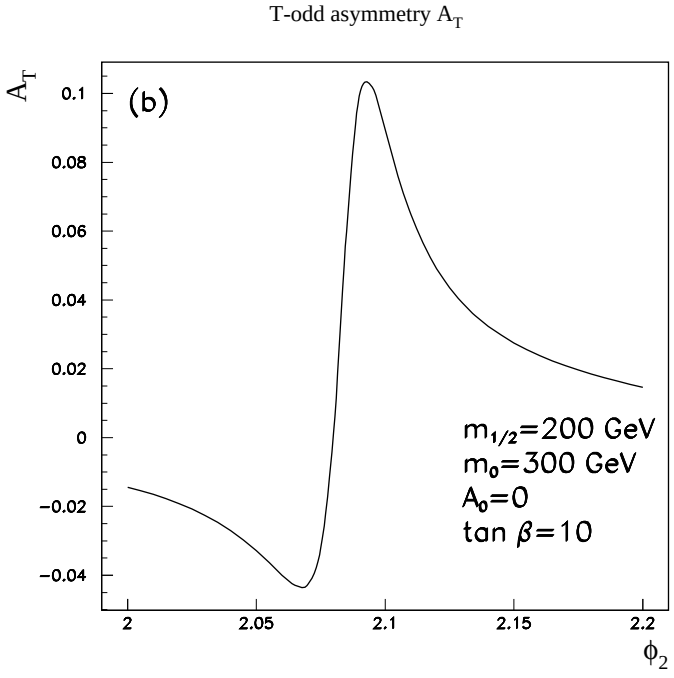

Fig. 25: *The T-violating asymmetry A_T in $\mu \to 3e$ decay is enhanced in the regions of parameter space shown in Fig. 24 where the branching ratio for $\mu \to e\gamma$ is suppressed, and different diagrams may interfere in the $\mu \to 3e$ decay amplitude [2].*

is suppressed [2]. If/when $\mu \to e\gamma$ and/or $\mu \to 3e$ decays are observed, measuring A_T (59) may provide an interesting window on CP violation in the seesaw model.

2.7 Lepton Electric Dipole Moments

This CP violation may also be visible in electric dipole moments for the electron and muon d_e and d_μ [91]. It is usually thought that these are unobservably small in the minimal supersymmetric seesaw model, and that $|d_e/d_\mu| = m_e/m_\mu$. However, d_e and d_μ may be strongly enhanced if the heavy singlet neutrinos are not degenerate [81], and depend on new phases that contribute to leptogenesis [2]. The leading contributions to d_e and d_μ in the presence of non-degenerate heavy-singlet neutrinos are produced by the following terms in the renormalization of soft supersymmetry-breaking parameters:

$$\begin{aligned} \left(\tilde{\delta} m_{\tilde{L}}^2\right)_{ij} &= \frac{18}{(4\pi)^4}\left(m_0^2 + A_e^2\right)\{Y_\nu^\dagger L Y_\nu, Y_\nu^\dagger Y_\nu\}_{ij} \ln\left(\frac{M_{GUT}}{\bar{M}}\right), \\ \left(\tilde{A}_e\right)_{ij} &= \frac{1}{(4\pi)^4} A_0 \left[11\{Y_\nu^\dagger L Y_\nu, Y_\nu^\dagger Y_\nu\} + 7[Y_\nu^\dagger L Y_\nu, Y_\nu^\dagger Y_\nu]\right]_{ij} \ln\left(\frac{M_{GUT}}{\bar{M}}\right), \end{aligned} \tag{62}$$

where the mean heavy-neutrino mass $\bar{M} \equiv \sqrt[3]{M_1 M_2 M_3}$ and the matrix $L \equiv \ln(\bar{M}/M_i)\delta_{ij}$ were introduced in (38).

It should be emphasized that non-degenerate heavy-singlet neutrinos are actually expected in most models of neutrino masses. Typical examples are texture models of the form

$$Y_\nu \sim Y_0 \begin{pmatrix} 0 & c\epsilon_\nu^3 & d\epsilon_\nu^3 \\ c\epsilon_\nu^3 & a\epsilon_\nu^2 & b\epsilon_\nu^2 \\ d\epsilon_\nu^3 & b\epsilon_\nu^2 & e^{i\psi} \end{pmatrix},$$

[2] This effect makes lepton electric dipole moments possible even in a two-generation model.

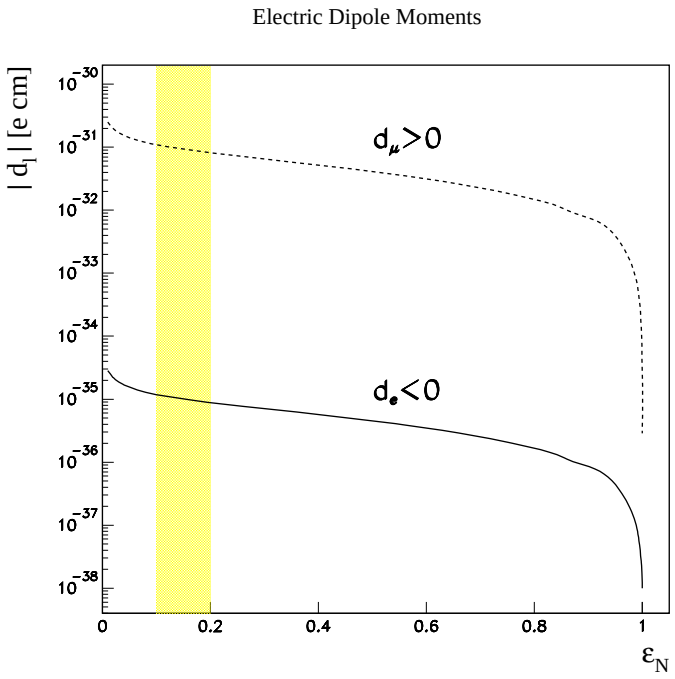

Fig. 26: *The electric dipole moments of the electron and muon, d_e and d_μ, may be enhanced if the heavy singlet neutrinos are non-degenerate. The horizontal axis parameterizes the breaking of their degeneracy, and the vertical strip indicates a range favoured in certain models [81].*

where Y_0 is an overall scale, ϵ_ν characterizes the hierarchy, a, b, c and d are $\mathcal{O}(1)$ complex numbers, and ψ is an arbitrary phase. For example, there is an SO(10) GUT model of this form with $d = 0$ and a flavour SU(3) model with $a = b$ and $c = d$. The hierarchy of heavy-neutrino masses in such a model is

$$M_1 : M_2 : M_3 \; = \; \epsilon_N^6 : \epsilon_N^4 : 1, \tag{63}$$

and indicative ranges of the hierarchy parameters are

$$\epsilon_\nu \sim \sqrt{\frac{\Delta m^2_{solar}}{\Delta m^2_{atmo}}} \; , \; \epsilon_N \sim 0.1 \text{ to } 0.2. \tag{64}$$

Fig. 26 shows how much d_e and d_μ may be increased as soon as the degeneracy between the heavy neutrinos is broken: $\epsilon \neq 1$. We also see that $|d_\mu/d_e| \gg m_\mu/m_e$ when $\epsilon_N \sim 0.1$ to 0.2. Scatter plots of d_e and d_μ are shown in Fig. 27, where we see that values as large as $d_\mu \sim 10^{-27}$ e.cm and $d_e \sim 3 \times 10^{-30}$ e.cm are possible. For comparison, the present experimental upper limits are $d_e < 1.6 \times 10^{-27}$ e.cm [92] and $d_\mu < 10^{-18}$ e.cm [25]. An ongoing series of experiments might be able to reach $d_e < 3 \times 10^{-30}$ e.cm, and a type of solid-state experiment that might be sensitive to $d_e \sim 10^{-33}$ e.cm has been proposed [93]. Also, $d_\mu \sim 10^{-24}$ e.cm might be accessible with the PRISM experiment proposed for the JHF [94], and $d_\mu \sim 5 \times 10^{-26}$ e.cm might be attainable at the front end of a neutrino factory [95]. It therefore seems that d_e might be measurable with foreseeable experiments, whilst d_μ would present more of a challenge.

2.8 (Not so) Rare Sparticle Decays

The suppression of rare lepton-flavour-violating (LFV) μ and τ decays in the supersymmetric seesaw model is due to loop effects and the small masses of the leptons relative to the sparticle mass scale. The

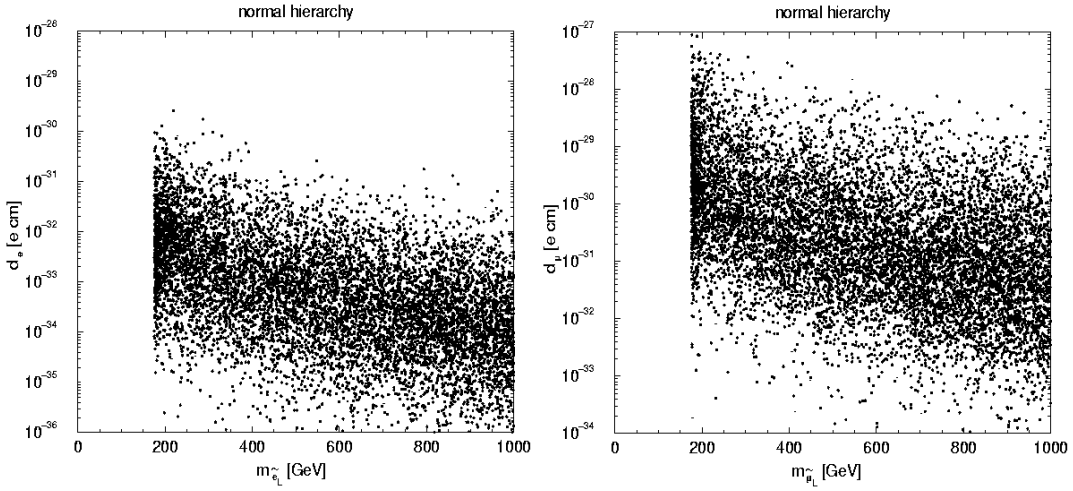

Fig. 27: *Scatter plots of d_e and d_μ in variants of the supersymmetric seesaw model, for different values of the unknown parameters [82].*

intrinsic slepton mixing may not be very small, in which case there might be relatively large amounts of LFV observable in sparticle decays. An example that might be detectable at the LHC is $\chi_2 \to \chi_1 \ell^\pm \ell'^\mp$, where $\chi_1(\chi_2)$ denotes the (next-to-)lightest neutralino [96]. The largest LFV effects might be in $\chi_2 \to \chi_1 \tau^\pm \mu^\mp$ and $\chi_2 \to \chi_1 \tau^\pm e^\mp$ [97], though $\chi_2 \to \chi_1 e^\pm \mu^\mp$ would be easier to detect.

As shown in Fig. 28 [97], these decays are likely to be enhanced in a region of CMSSM parameter space complementary to that where $\tau \to e/\mu\gamma$ decys are most copious. This is because the interesting $\chi_2 \to \chi_1 \tau^\pm \mu^\mp$ and $\chi_2 \to \chi_1 \tau^\pm e^\mp$ decays are mediated by slepton exchange, which is maximized when the slepton mass is close to m_{χ_1}. This happens in the coannihilation region where the LSP relic density may be in the range preferred by astrophysics and cosmology, even if m_{χ_1} is relatively large. Thus searches for LFV $\chi_2 \to \chi_1 \tau^\pm \mu^\mp$ and $\chi_2 \to \chi_1 \tau^\pm e^\mp$ decays are quite complementary to those for $\tau \to e/\mu\gamma$.

2.9 Possible CERN Projects beyond the LHC

What might come after the LHC at CERN? One possibility is the LHC itself, in the form of an energy or luminosity upgrade [98]. It seems that the possibilities for the former are very limited: a substantial energy upgrade would require a completely new machine in the LHC tunnel, with even higher-field magnets and new techniques for dealing with synchrotron radiation. On the other hand, a substantial increase in luminosity seems quite feasible, though it would require some rebuilding of (at least the central parts of) the LHC detectors.

The mainstream project for CERN after the LHC is CLIC, the multi-TeV linear e^+e^- collider [51]. CERN is continuing R&D on this project, with a view to being able to assess its feasibility when the LHC starts to produce data, e.g., specifying the energy scale of supersymmetry or extra dimensions. CLIC would complement the work of the LHC and any first-generation sub-TeV linear e^+e^- collider, e.g., by detailed studies of heavier sparticles such as heavier charginos, neutralinos and strongly-interacting sparticles [54, 52].

A possible alternative that has attracted considerable enthusiasm in Europe is to develop neutrino physics beyond the current CNGS project [99]. A first step might be an off-axis experiment in the CNGS beam, which could have interesting sensitivity to θ_{13} [100]. A second might be a super-beam produced by the SPL [101] at CERN and sent to a large detector in the Frjus tunnel [77]. A third step could be a storage ring for unstable ions, whose decays would produce a 'β beam' of pure ν_e or $\bar{\nu}_e$ neutrinos that could also be observed in a Fréjus experiment. These experiments might be able to measure δ via CP

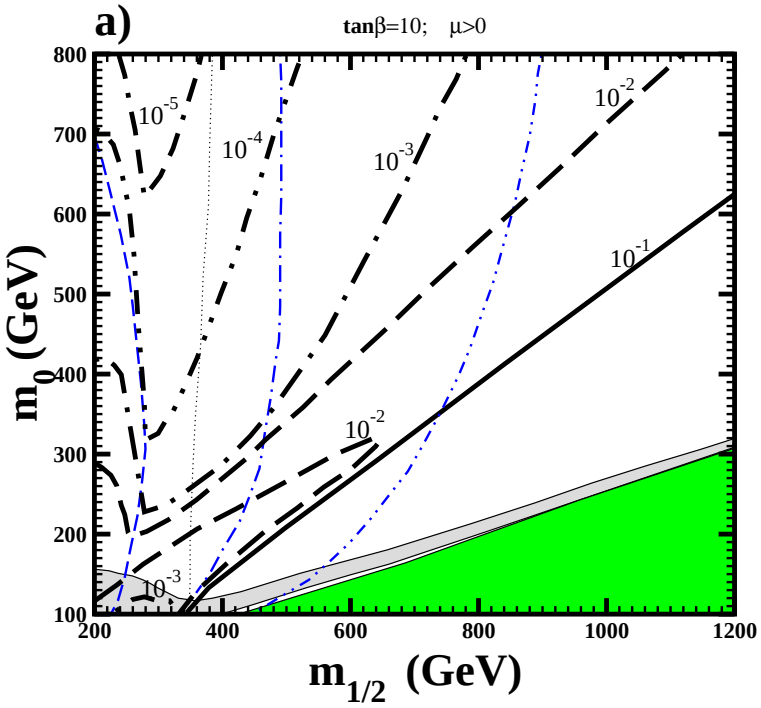

Fig. 28: *Contours of the possible ratio of the branching ratios for* $\chi_2 \to \chi_1 \tau^{\pm} \mu^{\mp}$ *and* $\chi_2 \to \chi_1 \mu^{\pm} \mu^{\mp}$ *(black lines) and of the branching ratio for* $\tau \to \mu\gamma$ *(near-vertical grey/blue lines). [97].*

and/or T violation in neutrino oscillations [102]. A fourth step could be a full-fledged neutrino factory based on a muon storage ring, which would produce pure ν_μ and $\bar{\nu}_e$ (or ν_e and $\bar{\nu}_\mu$ beams and provide a greatly enhanced capability to search for or measure δ via CP violation in neutrino oscillations [95]. Further steps might then include $\mu^+\mu^-$ colliders with various centre-of-mass energies, from the mass of the lightest Higgs boson, through those of the heavier MSSM Higgs bosons H, A, to the multi-TeV energy frontier [103].

This is an ambitious programme that requires considerable R&D. CERN currently does not have the financial resources to support this, but it is hoped that other European laboratories and the European Union might support a network of interested physicists. Such an ambitious neutrino programme would also require wide support in the physics community. In addition to the neutrino physics itself, many might find enticing the other experimental possibilities offered by the type of intense proton driver required. These could include some of the topics discussed in this Lecture, including rare decays of slow or stopped muons [95], such as $\mu \to e\gamma$ and anomalous $\mu \to e$ conversion on a nucleus, measurements of $g_\mu - 2$ and d_μ, rare K decays [104], short-baseline deep-inelastic neutrino experiments with very intense beams [105], muonic atoms, etc., etc.. Physicists interested in such a programme, which nicely complements the 'core business' of the neutrino factory, should get together and see how a coalition of interested parties could be assembled. A large investment in neutrino physics will require a broad range of support.

References

[1] J. R. Ellis, Lectures at 1998 CERN Summer School, St. Andrews, *Beyond the Standard Model for Hillwalkers*, arXiv:hep-ph/9812235.

[2] J. R. Ellis, J. Hisano, S. Lola and M. Raidal, Nucl. Phys. B **621**, 208 (2002) [arXiv:hep-ph/0109125].

[3] J. R. Ellis, *The Superstring: Theory Of Everything, Or Of Nothing?*, Nature **323** (1986) 595.

[4] L. Maiani, *Proceedings of the 1979 Gif-sur-Yvette Summer School On Particle Physics*, 1; G. 't Hooft, in *Recent Developments in Gauge Theories, Proceedings of the Nato Advanced Study Institute, Cargese, 1979*, eds. G. 't Hooft *et al.*, (Plenum Press, NY, 1980); E. Witten, Phys. Lett. B **105** (1981) 267.

[5] J. Ellis, S. Kelley and D. V. Nanopoulos, Phys. Lett. B **260** (1991) 131; U. Amaldi, W. de Boer and H. Furstenau, Phys. Lett. B **260** (1991) 447; P. Langacker and M. x. Luo, Phys. Rev. D **44** (1991) 817; C. Giunti, C. W. Kim and U. W. Lee, Mod. Phys. Lett. A **6** (1991) 1745.

[6] M. B. Green, J. H. Schwarz and E. Witten, *Superstring Theory*, (Cambridge Univ. Press, 1987).

[7] J. R. Ellis, Lectures at 2001 CERN Summer School, Beatenberg, *Supersymmetry for Alp hikers*, arXiv:hep-ph/0203114.

[8] S. Ferrara, J. Wess and B. Zumino, Phys. Lett. B **51** (1974) 239; S. Ferrara, J. Iliopoulos and B. Zumino, Nucl. Phys. B **77** (1974) 413.

[9] P. Fayet, as reviewed in *Supersymmetry, Particle Physics And Gravitation*, CERN-TH-2864, published in *Proc. of Europhysics Study Conf. on Unification of Fundamental Interactions*, Erice, Italy, Mar 17-24, 1980, eds. S. Ferrara, J. Ellis, P. van Nieuwenhuizen (Plenum Press, 1980).

[10] LEP Electroweak Working Group, `http://lepewwg.web.cern.ch/LEPEWWG/Welcome.html`.

[11] Y. Okada, M. Yamaguchi and T. Yanagida, Prog. Theor. Phys. **85** (1991) 1; J. R. Ellis, G. Ridolfi and F. Zwirner, Phys. Lett. B **257** (1991) 83; H. E. Haber and R. Hempfling, Phys. Rev. Lett. **66** (1991) 1815.

[12] J. Ellis, J.S. Hagelin, D.V. Nanopoulos, K.A. Olive and M. Srednicki, Nucl. Phys. B **238** (1984) 453; see also H. Goldberg, Phys. Rev. Lett. **50** (1983) 1419.

[13] For an early review, see: P. Fayet and S. Ferrara, Phys. Rept. **32** (1977) 249; see also: H. P. Nilles, Phys. Rept. **110** (1984) 1; H. E. Haber and G. L. Kane, Phys. Rept. **117** (1985) 75.

[14] J. R. Ellis and D. V. Nanopoulos, Phys. Lett. B **110** (1982) 44; R. Barbieri and R. Gatto, Phys. Lett. B **110** (1982) 211.

[15] K. Inoue, A. Kakuto, H. Komatsu and S. Takeshita, Prog. Theor. Phys. **68** (1982) 927 [Erratum-ibid. **70** (1982) 330]; L.E. Ibáñez and G.G. Ross, Phys. Lett. B **110** (1982) 215; L.E. Ibáñez, Phys. Lett. B **118** (1982) 73; J. Ellis, D.V. Nanopoulos and K. Tamvakis, Phys. Lett. B **121** (1983) 123; J. Ellis, J. Hagelin, D.V. Nanopoulos and K. Tamvakis, Phys. Lett. B **125** (1983) 275; L. Alvarez-Gaumé, J. Polchinski, and M. Wise, Nucl. Phys. B **221** (1983) 495.

[16] Joint LEP 2 Supersymmetry Working Group, *Combined LEP Chargino Results, up to 208 GeV*, `http://lepsusy.web.cern.ch/lepsusy/www/inos_moriond01/charginos_pub.html`.

[17] Joint LEP 2 Supersymmetry Working Group, *Combined LEP Selectron/Smuon/Stau Results, 183-208 GeV*, `http://alephwww.cern.ch/~ganis/SUSYWG/SLEP/sleptons_2k01.html`.

[18] J. R. Ellis, T. Falk, G. Ganis, K. A. Olive and M. Srednicki, Phys. Lett. B **510** (2001) 236 [arXiv:hep-ph/0102098].

[19] LEP Higgs Working Group for Higgs boson searches, OPAL Collaboration, ALEPH Collaboration, DELPHI Collaboration and L3 Collaboration, *Search for the Standard Model Higgs Boson at LEP*, ALEPH-2001-066, DELPHI-2001-113, CERN-L3-NOTE-2699, OPAL-PN-479, LHWG-NOTE-2001-03, CERN-EP/2001-055, arXiv:hep-ex/0107029; *Searches for the neutral Higgs bosons of the MSSM: Preliminary combined results using LEP data collected at energies up to 209 GeV*, LHWG-NOTE-2001-04, ALEPH-2001-057, DELPHI-2001-114, L3-NOTE-2700, OPAL-TN-699, arXiv:hep-ex/0107030.

[20] M.S. Alam et al., [CLEO Collaboration], Phys. Rev. Lett. **74** (1995) 2885 as updated in S. Ahmed et al., CLEO CONF 99-10; BELLE Collaboration, BELLE-CONF-0003, contribution to the 30th International conference on High-Energy Physics, Osaka, 2000. See also K. Abe *et al.*, [Belle Collaboration], [arXiv:hep-ex/0107065]; L. Lista [BaBar Collaboration], [arXiv:hep-ex/0110010]; C. Degrassi, P. Gambino and G. F. Giudice, JHEP **0012** (2000) 009 [arXiv:hep-ph/0009337]; M. Carena, D. Garcia, U. Nierste and C. E. Wagner, Phys. Lett. B **499** (2001) 141 [arXiv:hep-ph/0010003].

[21] J. R. Ellis, K. A. Olive and Y. Santoso, New J. Phys. **4** (2002) 32 [arXiv:hep-ph/0202110].

[22] M. Carena, J. R. Ellis, A. Pilaftsis and C. E. Wagner, Nucl. Phys. B **586** (2000) 92 [arXiv:hep-ph/0003180], Phys. Lett. B **495** (2000) 155 [arXiv:hep-ph/0009212]; and references therein.

[23] J. R. Ellis, G. Ganis, D. V. Nanopoulos and K. A. Olive, Phys. Lett. B **502** (2001) 171 [arXiv:hep-ph/0009355].

[24] S. Heinemeyer, W. Hollik and G. Weiglein, Comput. Phys. Commun. **124**, 76 (2000) [arXiv:hep-ph/9812320]; S. Heinemeyer, W. Hollik and G. Weiglein, Eur. Phys. J. C **9** (1999) 343 [arXiv:hep-ph/9812472].

[25] H. N. Brown *et al.* [Muon g-2 Collaboration], Phys. Rev. Lett. **86**, 2227 (2001) [arXiv:hep-ex/0102017].

[26] G. W. Bennett *et al.* [Muon g-2 Collaboration], ppm," Phys. Rev. Lett. **89** (2002) 101804 [Erratum-ibid. **89** (2002) 129903] [arXiv:hep-ex/0208001].

[27] M. Davier, S. Eidelman, A. Hocker and Z. Zhang, arXiv:hep-ph/0208177; see also K. Hagiwara, A. D. Martin, D. Nomura and T. Teubner, arXiv:hep-ph/0209187; F. Jegerlehner, unpublished, as reported in M. Krawczyk, arXiv:hep-ph/0208076.

[28] M. Knecht and A. Nyffeler, arXiv:hep-ph/0111058; M. Knecht, A. Nyffeler, M. Perrottet and E. De Rafael, arXiv:hep-ph/0111059; M. Hayakawa and T. Kinoshita, arXiv:hep-ph/0112102; I. Blokland, A. Czarnecki and K. Melnikov, arXiv:hep-ph/0112117; J. Bijnens, E. Pallante and J. Prades, arXiv:hep-ph/0112255.

[29] L. L. Everett, G. L. Kane, S. Rigolin and L. Wang, Phys. Rev. Lett. **86**, 3484 (2001) [arXiv:hep-ph/0102145]; J. L. Feng and K. T. Matchev, Phys. Rev. Lett. **86**, 3480 (2001) [arXiv:hep-ph/0102146]; E. A. Baltz and P. Gondolo, Phys. Rev. Lett. **86**, 5004 (2001) [arXiv:hep-ph/0102147]; U. Chattopadhyay and P. Nath, Phys. Rev. Lett. **86**, 5854 (2001) [arXiv:hep-ph/0102157]; S. Komine, T. Moroi and M. Yamaguchi, Phys. Lett. B **506**, 93 (2001) [arXiv:hep-ph/0102204]; J. Ellis, D. V. Nanopoulos and K. A. Olive, Phys. Lett. B **508** (2001) 65 [arXiv:hep-ph/0102331]; R. Arnowitt, B. Dutta, B. Hu and Y. Santoso, Phys. Lett. B **505** (2001) 177 [arXiv:hep-ph/0102344] S. P. Martin and J. D. Wells, Phys. Rev. D **64**, 035003 (2001) [arXiv:hep-ph/0103067]; H. Baer, C. Balazs, J. Ferrandis and X. Tata, Phys. Rev. D **64**, 035004 (2001) [arXiv:hep-ph/0103280].

[30] N. A. Bahcall, J. P. Ostriker, S. Perlmutter and P. J. Steinhardt, Science **284** (1999) 1481 [arXiv:astro-ph/9906463].

[31] S. Mizuta and M. Yamaguchi, Phys. Lett. B **298** (1993) 120 [arXiv:hep-ph/9208251]; J. Edsjo and P. Gondolo, Phys. Rev. D **56** (1997) 1879 [arXiv:hep-ph/9704361].

[32] J. Ellis, T. Falk and K. A. Olive, Phys. Lett. B **444** (1998) 367 [arXiv:hep-ph/9810360]; J. Ellis, T. Falk, K. A. Olive and M. Srednicki, Astropart. Phys. **13** (2000) 181 [arXiv:hep-ph/9905481]; M. E. Gómez, G. Lazarides and C. Pallis, Phys. Rev. D **61** (2000) 123512 [arXiv:hep-ph/9907261] and Phys. Lett. B **487** (2000) 313 [arXiv:hep-ph/0004028]; R. Arnowitt, B. Dutta and Y. Santoso, Nucl. Phys. B **606** (2001) 59 [arXiv:hep-ph/0102181].

[33] C. Boehm, A. Djouadi and M. Drees, Phys. Rev. D **62** (2000) 035012 [arXiv:hep-ph/9911496].

[34] J. Ellis, K.A. Olive and Y. Santoso, arXiv:hep-ph/0112113.

[35] M. Drees and M. M. Nojiri, Phys. Rev. D **47** (1993) 376 [arXiv:hep-ph/9207234]; H. Baer and M. Brhlik, Phys. Rev. D **53** (1996) 597 [arXiv:hep-ph/9508321] and Phys. Rev. D **57** (1998) 567 [arXiv:hep-ph/9706509]; H. Baer, M. Brhlik, M. A. Diaz, J. Ferrandis, P. Mercadante, P. Quintana and X. Tata, Phys. Rev. D **63** (2001) 015007 [arXiv:hep-ph/0005027]; A. B. Lahanas, D. V. Nanopoulos and V. C. Spanos, Mod. Phys. Lett. A **16** (2001) 1229 [arXiv:hep-ph/0009065].

[36] J. L. Feng, K. T. Matchev and T. Moroi, Phys. Rev. Lett. **84**, 2322 (2000) [arXiv:hep-ph/9908309]; J. L. Feng, K. T. Matchev and T. Moroi, Phys. Rev. D **61**, 075005 (2000) [arXiv:hep-ph/9909334]; J. L. Feng, K. T. Matchev and F. Wilczek, Phys. Lett. B **482**, 388 (2000) [arXiv:hep-ph/0004043].

[37] J. R. Ellis and K. A. Olive, Phys. Lett. B **514** (2001) 114 [arXiv:hep-ph/0105004].

[38] For other recent calculations, see, for example: A. B. Lahanas, D. V. Nanopoulos and V. C. Spanos, Phys. Lett. B **518** (2001) 94 [arXiv:hep-ph/0107151]; V. Barger and C. Kao, Phys. Lett. B **518**, 117 (2001) [arXiv:hep-ph/0106189]; L. Roszkowski, R. Ruiz de Austri and T. Nihei, JHEP **0108**, 024 (2001) [arXiv:hep-ph/0106334]; A. Djouadi, M. Drees and J. L. Kneur, JHEP **0108**, 055 (2001) [arXiv:hep-ph/0107316].

[39] J. Ellis, K. Enqvist, D. V. Nanopoulos and F. Zwirner, Mod. Phys. Lett. A **1**, 57 (1986); R. Barbieri and G. F. Giudice, Nucl. Phys. B **306** (1988) 63.

[40] M. Battaglia *et al.*, Eur. Phys. J. C **22** (2001) 535 [arXiv:hep-ph/0106204].

[41] G. L. Kane, J. Lykken, S. Mrenna, B. D. Nelson, L. T. Wang and T. T. Wang, arXiv:hep-ph/0209061.

[42] D. R. Tovey, Phys. Lett. B **498** (2001) 1 [arXiv:hep-ph/0006276].

[43] F. E. Paige, hep-ph/0211017.

[44] ATLAS Collaboration, *ATLAS detector and physics performance Technical Design Report*, CERN/LHCC 99-14/15 (1999); S. Abdullin *et al.* [CMS Collaboration], arXiv:hep-ph/9806366; S. Abdullin and F. Charles, Nucl. Phys. B **547** (1999) 60 [arXiv:hep-ph/9811402]; CMS Collaboration, Technical Proposal, CERN/LHCC 94-38 (1994).

[45] D. Denegri, W. Majerotto and L. Rurua, Phys. Rev. D **60** (1999) 035008.

[46] I. Hinchliffe, F. E. Paige, M. D. Shapiro, J. Soderqvist and W. Yao, Phys. Rev. D **55** (1997) 5520;

[47] TESLA Technical Design Report, DESY-01-011, Part III, *Physics at an e^+e^- Linear Collider* (March 2001).

[48] J. Ellis, S. Heinemeyer, K. A. Olive and G. Weiglein, preprint CERN–TH/2002-289, in preparation.

[49] J. R. Ellis, G. Ganis and K. A. Olive, Phys. Lett. B **474** (2000) 314 [arXiv:hep-ph/9912324].

[50] G. A. Blair, W. Porod and P. M. Zerwas, Phys. Rev. **D63** (2001) 017703 [arXiv:hep-ph/0007107]; arXiv:hep-ph/0210058.

[51] R. W. Assmann *et al.* [CLIC Study Team], *A 3-TeV e^+e^- Linear Collider Based on CLIC Technology*, ed. G. Guignard, CERN 2000-08; for more information about this project, see: `http://ps-div.web.cern.ch/ps-div/CLIC/Welcome.html`.

[52] CLIC Physics Study Group, `http://clicphysics.web.cern.ch/CLICphysics/`.

[53] For more information about this project, see: `http://ctf3.home.cern.ch/ctf3/CTFindex.htm`.

[54] M. Battaglia, private communication.

[55] J. Ellis, J. L. Feng, A. Ferstl, K. T. Matchev and K. A. Olive, arXiv:astro-ph/0110225.

[56] CDMS Collaboration, R. W. Schnee *et al.*, Phys. Rept. **307**, 283 (1998).

[57] CRESST Collaboration, M. Bravin *et al.*, Astropart. Phys. **12**, 107 (1999) [arXiv:hep-ex/9904005].

[58] H. V. Klapdor-Kleingrothaus, arXiv:hep-ph/0104028.

[59] DAMA Collaboration, R. Bernabei *et al.*, Phys. Lett. B **436** (1998) 379.

[60] G. Jungman, M. Kamionkowski and K. Griest, Phys. Rept. **267**, 195 (1996) [arXiv:hep-ph/9506380]; `http://t8web.lanl.gov/people/jungman/neut-package.html`.

[61] See also the lectures at this school by W. J. Marciano.

[62] Y. Fukuda *et al.* [Super-Kamiokande Collaboration], Phys. Rev. Lett. **81**, 1562 (1998) [arXiv:hep-ex/9807003].

[63] Q. R. Ahmad *et al.* [SNO Collaboration], Phys. Rev. Lett. **89** (2002) 011301 [arXiv:nucl-ex/0204008]; Phys. Rev. Lett. **89** (2002) 011302 [arXiv:nucl-ex/0204009].

[64] R. Barbieri, J. R. Ellis and M. K. Gaillard, Phys. Lett. B **90** (1980) 249.

[65] M. Gell-Mann, P. Ramond and R. Slansky, Proceedings of the Supergravity Stony Brook Workshop, New York, 1979, eds. P. Van Nieuwenhuizen and D. Freedman (North-Holland, Amsterdam); T. Yanagida, Proceedings of the Workshop on Unified Theories and Baryon Number in the Universe, Tsukuba, Japan 1979 (edited by A. Sawada and A. Sugamoto, KEK Report No. 79-18, Tsukuba); R. Mohapatra and G. Senjanovic, Phys. Rev. Lett. **44** (1980) 912.

[66] P. H. Frampton, S. L. Glashow and T. Yanagida, arXiv:hep-ph/0208157.

[67] T. Endoh, S. Kaneko, S. K. Kang, T. Morozumi and M. Tanimoto, arXiv:hep-ph/0209020.

[68] J. R. Ellis, J. S. Hagelin, S. Kelley and D. V. Nanopoulos, Nucl. Phys. B **311** (1988) 1.

[69] J. R. Ellis, M. E. Gómez, G. K. Leontaris, S. Lola and D. V. Nanopoulos, Eur. Phys. J. C **14** (2000) 319.

[70] J. R. Ellis, M. K. Gaillard and D. V. Nanopoulos, Nucl. Phys. B **109** (1976) 213.

[71] M. Kobayashi and T. Maskawa, Prog. Theor. Phys. **49** (1973) 652.

[72] Z. Maki, M. Nakagawa and S. Sakata, Prog. Theor. Phys. **28** (1962) 870.

[73] S. Fukuda *et al.* [Super-Kamiokande Collaboration], Phys. Lett. B **539** (2002) 179 [arXiv:hep-ex/0205075].

[74] Chooz Collaboration, Phys. Lett. B **420** (1998) 397.

[75] A. De Rújula, M.B. Gavela and P. Hernández, Nucl. Phys. **B547** (1999) 21, hep-ph/9811390.

[76] A. Cervera *et al.*, Nucl. Phys. B **579**, 17 (2000) [Erratum-ibid. B **593**, 731 (2001)].

[77] M. Apollonio *et al.*, *Oscillation physics with a neutrino factory*, arXiv:hep-ph/0210192; and references therein.

[78] J. A. Casas and A. Ibarra, Nucl. Phys. B **618** (2001) 171 [arXiv:hep-ph/0103065].

[79] M. Fukugita and T. Yanagida, Phys. Lett. **B174**, 45 (1986).

[80] S. Davidson and A. Ibarra, JHEP **0109** (2001) 013.

[81] J. R. Ellis, J. Hisano, M. Raidal and Y. Shimizu, Phys. Lett. B **528**, 86 (2002) [arXiv:hep-ph/0111324].

[82] J. R. Ellis, J. Hisano, M. Raidal and Y. Shimizu, arXiv:hep-ph/0206110.

[83] J. R. Ellis and M. Raidal, Nucl. Phys. B **643** (2002) 229 [arXiv:hep-ph/0206174].

[84] A. Masiero and O. Vives, New J. Phys. **4** (2002) 4.

[85] C. Jarlskog, Phys. Rev. Lett. **55** (1985) 1039; Z. Phys. C **29** (1985) 491.

[86] K. Hagiwara *et al.* [Particle Data Group Collaboration], Phys. Rev. D **66** (2002) 010001.

[87] R. Cyburt, J. R. Ellis, B. Fields and K. A. Olive, preprint CERN-TH/2002-207, in preparation, and references therein.

[88] J. R. Ellis, M. Raidal and T. Yanagida, arXiv:hep-ph/0206300.

[89] Y. Kuno and Y. Okada, Rev. Mod. Phys. **73** (2001) 151; J. Hisano, T. Moroi, K. Tobe and M. Yamaguchi, Phys. Rev. D **53** (1996) 2442; J. Hisano, D. Nomura and T. Yanagida, Phys. Lett. B **437** (1998) 351; J. Hisano and D. Nomura, Phys. Rev. D **59** (1999) 116005; W. Buchmüller, D. Delepine and F. Vissani, Phys. Lett. B **459** (1999) 171; M. E. Gómez, G. K. Leontaris, S. Lola and J. D. Vergados, Phys. Rev. D **59** (1999) 116009; W. Buchmüller, D. Delepine and L. T. Handoko, Nucl. Phys. B **576** (2000) 445; J. L. Feng, Y. Nir and Y. Shadmi, Phys. Rev. D **61** (2000) 113005; J. Sato and K. Tobe, Phys. Rev. D **63** (2001) 116010; J. Hisano and K. Tobe, Phys. Lett. B **510** (2001) 197; D. Carvalho, J. Ellis, M. Gómez and S. Lola, Phys. Lett. B **515** (2001) 323; S. Baek, T. Goto, Y. Okada and K. Okumura, hep-ph/0104146; S. Lavignac, I. Masina and C.A. Savoy, hep-ph/0106245.

[90] Y. Okada, K. Okumura and Y. Shimizu, Phys. Rev. D **58** (1998) 051901; Phys. Rev. D **61** (2000) 094001.

[91] T. Ibrahim and P. Nath, Phys. Rev. D **57** (1998) 478 [Erratum - *ibid.* **58** (1998) 019901]; S. Abel, S. Khalil and O. Lebedev, Nucl. Phys. B **606** (2001) 151; S. Abel, D. Bailin, S. Khalil and O. Lebedev, Phys. Lett. B **504** (2001) 241.

[92] B. C. Regan, E. D. Commins, C. J. Schmidt and D. DeMille, Phys. Rev. Lett. **88** (2002) 071805.

[93] S. K. Lamoreaux, arXiv:nucl-ex/0109014.

[94] M. Furusaka *et al.*, JAERI/KEK Joint Project Proposal *The Joint Project for High-Intensity Proton Accelerators*, KEK-REPORT-99-4, JAERI-TECH-99-056.

[95] J. Äystö *et al.*, *Physics with Low-Energy Muons at a Neutrino Factory Complex*, CERN-TH/2001-231, hep-ph/0109217; and references therein.

[96] I. Hinchliffe and F. E. Paige, Phys. Rev. D **63** (2001) 115006 [arXiv:hep-ph/0010086].

[97] D. F. Carvalho, J. R. Ellis, M. E. Gómez, S. Lola and J. C. Romao, arXiv:hep-ph/0206148.

[98] F. Gianotti *et al.*, *Physics potential and experimental challenges of the LHC luminosity upgrade*, arXiv:hep-ph/0204087.

[99] For more information about this project, see:
`http://proj-cngs.web.cern.ch/proj-cngs/`; for the experiments, see:
OPERA Collaboration, `http://operaweb.web.cern.ch/operaweb/index.shtml`;
ICARUS Collaboration, `http://www.aquila.infn.it/icarus/`.

[100] F. Dydak, private communication.

[101] B. Autin *et al.*, CERN report CERN-2000-012 (2000).

[102] P. Zucchelli, Phys. Lett. **B532** 166 (2002).

[103] Neutrino Factory and Muon Collider Collaboration,
`http://www.cap.bnl.gov/mumu/mu_home_page.html`;
European Muon Working Groups,
`http://muonstoragerings.cern.ch/Welcome.html`.

[104] A. Belyaev *et al.* [Kaon Physics Working Group Collaboration], *Kaon physics with a high-intensity proton driver*, arXiv:hep-ph/0107046.

[105] M. L. Mangano *et al.*, *Physics at the front-end of a neutrino factory: A quantitative appraisal*, arXiv:hep-ph/0105155.